International Ocean Discovery Program Expedition 389 Preliminary Report

Hawaiian Drowned Reefs

Platform operations 31 August–31 October 2023

Onshore Science Party 6–26 February 2024

Jody M. Webster, Ana Christina Ravelo, Hannah L.J. Grant, and the Expedition 389 Scientists

Citation

Webster, J.M., Ravelo, A.C., Grant, H.L.J., and the Expedition 389 Scientists, 2024. Expedition 389 Preliminary Report: Hawaiian Drowned Reefs. International Ocean Discovery Program. https://doi.org/10.14379/iodp.pr.389.2024

Expedition 389 participants

Expedition 389 scientists

Jody M. Webster
Co-Chief Scientist
School of Geosciences, Geocoastal Research Group
University of Sydney
Australia
jody.webster@sydney.edu.au

Ana Christina Ravelo
Co-Chief Scientist
Ocean Sciences Department, Institute of Marine Sciences
University of California Santa Cruz
USA
acr@ucsc.edu

Hannah L. J. Grant
Lead Expedition Project Manager
British Geological Survey
The Lyell Centre
United Kingdom
hgrant@bgs.ac.uk

Margaret Stewart
Expedition Project Manager
British Geological Survey
The Lyell Centre
United Kingdom
mstewart@bgs.ac.uk

Marisa Rydzy
Petrophysics Staff Scientist
Department of Geology, Geography and the Environment
University of Leicester
United Kingdom
mbr8@bgs.ac.uk

Erwan Le Ber
Senior Petrophysicist and EPM support
Géosciences Montpellier
Université de Montpellier
France
erwan.le-ber@umontpellier.fr

Nicola Allison
Inorganic Geochemist
Scottish Oceans Institute
University of St. Andrews
United Kingdom
na9@st-andrews.ac.uk

Ryuji Asami
Inorganic Geochemist
Department of Earth Science
Tohoku University
Japan
ryuji.asami.b5@tohoku.ac.jp

Brian Boston
Physical Properties Specialist
Department of Geosciences
Auburn University
USA
boston@auburn.edu

Juan Carlos Braga
Coralline Algal Specialist
Department of Stratigraphy and Paleontology
Universidad de Granada
Spain
jbraga@ugr.es

Logan Brenner
Inorganic Geochemist
Environmental Science
Barnard College
USA
lbrenner@barnard.edu

Xuefei Chen
Inorganic Geochemist
Guangzhou Institute of Geochemistry
Chinese Academy of Sciences
State Key Laboratory of Isotope Geochemistry
China
chenxf@gig.ac.cn

Peter Chutcharavan
Inorganic Geochemist
Earth and Environmental Sciences
University of Minnesota Twin Cities
USA

Present affiliation (4 April 2024):
Division of Environmental Health Sciences
Wadsworth Center
New York State Department of Health
USA
peter.chutcharavan@health.ny.gov

Andrea Dutton
Inorganic Geochemist
Department of Geoscience
University of Wisconsin—Madison
USA
dutton3@wisc.edu

Thomas Felis
Inorganic Geochemist
MARUM—Center for Marine Environmental Sciences
University of Bremen
Germany
tfelis@marum.de

Naoto Fukuyo
Paleomagnetist
Geological Survey of Japan
National Institute of Advanced Industrial Science and Technology
Japan
naoto.hooke@gmail.com

Eberhard Gischler
Sedimentologist
Goethe-University Frankfurt
Germany
gischler@em.uni-frankfurt.de

Sahra Greve
Inorganic Geochemist
Institute for Environmental Physics
University of Heidelberg
Germany
sahra.greve@stud.uni-heidelberg.de

Amy Hagen
Inorganic Geochemist
Department of Geosciences
Virginia Tech
USA
amyhagen@vt.edu

Youri Hamon
Sedimentologist
IFP Energies Nouvelles (IFPEN)
France
youri.hamon@ifpen.fr

Ed Hathorne
Inorganic Geochemist
GEOMAR Helmholtz Centre for Ocean Research
Germany
ehathorne@geomar.de

Marc Humblet
Coral Specialist
Department of Earth and Planetary Sciences
Nagoya University
Japan
humblet.marc.n3@f.mail.nagoya-u.ac.jp

Stephan Jorry
Physical Properties Specialist
Geo-Ocean, Technopole La Pointe du Diable
IFREMER
France
stephan.jorry@ifremer.fr

Pankaj Khanna
Sedimentologist
Earth Science
IIT Gandhinagar
India
Pankaj.khanna@iitgn.ac.in

Helen McGregor
Inorganic Geochemist
School of Earth, Atmospheric and Life Sciences
University of Wollongong
Australia
mcgregor@uow.edu.au

Richard Mortlock
Inorganic Geochemist
Earth and Planetary Sciences
Rutgers University
USA
rmortloc@eps.rutgers.edu

Theresa Nohl
Sedimentologist
Department of Palaeontology
University of Vienna
Austria
theresa.nohl@univie.ac.at

Donald Potts
Coral Specialist
Ecology and Evolutionary Biology Department
University of California Santa Cruz
USA
potts@ucsc.edu

Ana Prohaska
Microbiologist
Globe Institute
University of Copenhagen
Denmark
ana.prohaska@sund.ku.dk

Nancy Prouty
Inorganic Geochemist
Pacific Coastal and Marine Sciences
U.S. Geological Survey
USA
nprouty@usgs.gov

Willem Renema
Micropaleontologist (benthic foraminifers)
Institute for Biodiversity and Ecosystem Dynamics
Naturalis Biodiversity Center
Netherlands
willem.renema@naturalis.nl

Kenna Harmony Rubin
Inorganic Geochemist
Department of Earth Sciences
University of Hawaii at Manoa
USA

Present address (4 April 2024):
Graduate School of Oceanography
University of Rhode Island
USA
kenna.rubin@uri.edu

Hildegard Westphal
Sedimentologist
Leibniz-Zentrum für Marine Tropenforschung (ZMT)
University of Bremen
Germany
hildegard.westphal@leibniz-zmt.de

Yusuke Yokoyama
Inorganic Geochemist
Atmosphere and Ocean Research Institute
The University of Tokyo
Japan
yokoyama@aori.u-tokyo.ac.jp

Outreach

Ulrike Prange
ECORD Science Operator Outreach Manager/Media Relations
Germany
uprange@marum.de

Marley Parker
Onboard Outreach Officer
USA
mlparkermedia@gmail.com

Operational, management, and technical staff

ESO personnel and technical representatives

Ursula Röhl
Onshore Operations Manager/Laboratory and Curation Manager

Graham Tulloch
Operations Manager

Vera B. Bender
Data Manager

Oliver Blasczcyk
IT Specialist

Liane Brück
Geophysics Technician

Volker Diekamp
Photographer

Alan Douglas
IT and Network Support

Thomas Frederichs
Paleomagnetist

Patrizia Gepraegs
Core Curator/Assistant Laboratory Manager

Tayyaba Khurram
Petrophysics Technician

Brit Kokisch
Sedimentology Technician/LECO Operator

Martin Kölling
Inorganic Geochemistry Laboratory Manager

Holger Kuhlmann
Core Curator/IODP Bremen Core Repository Superintendent

Vera Lukies
Petrophysics Technician

Andrew McIntyre
Petrophysicist

Mary Mowat
Data Manager

Walid Naciri
Petrophysics Technician

Silvana Pape
Inorganic Geochemistry Laboratory Technician

Luzie Schnieders
Geochemist

Nina Rohlfs
Core Curator/Logistics

Christoph Vogt
XRD Laboratory Manager

Tim Van Peer
Petrophysicist

Alex Wülbers
Core Curator/Logistics

Core scanning

Jeremy Everest
British Geological Survey Core Scanning Facility/ESO EPM

Mark Fellgett
British Geological Survey Core Scanning Facility

Cameron Fletcher
British Geological Survey Core Scanning Facility

Philip Neep
British Geological Survey Core Scanning Facility

Jason Ngui
British Geological Survey Core Scanning Facility

Dave Morgan
British Geological Survey Core Scanning Facility

Max Page
British Geological Survey Core Scanning Facility

Owen Rathbone
British Geological Survey Core Scanning Facility

Kotryna Savickaite
British Geological Survey Core Scanning Facility

Elisabeth Steer
British Geological Survey Core Scanning Facility

Beata Sternal
British Geological Survey Core Scanning Facility

Adrian White
British Geological Survey Core Scanning Facility

Atilla Basoglu
TheiaX

Cecilia Contreras
TheiaX

Erik Herrmann
TheiaX

Laura Tusa
TheiaX

Benthic

George Uller
Benthic Project Manager

Neil Laird
Offshore Manager

Michael Serra
Offshore Manager

Chloe Easterling
Medic

Sean MacRae
Superintendent

Michael Quirk
Superintendent

Richard Irving
Supervisor

Graeme Love
Supervisor

Ben Wallinger
Supervisor

Chris Boxall
PROD Operator/Assistant Superintendent

Nathan Bennett
PROD Operator

Stephen Bellin
PROD Operator

Luke Bettinger
PROD Operator

Warren Brunke
PROD Operator

Luis Chapa
PROD Operator

James Davenport
PROD Operator

George Gottschall
PROD Operator

Charles Gonzalez
PROD Operator

Kenneth Neilson
PROD Operator

Barbara Azevedo
Lead Geo Engineer

Dylan Kuipersmith
Lead Geo Engineer

Andre Alves
Benthic Geo Engineer

Deepak Kalla
Benthic Geo Engineer

Leonel Mello
Benthic Geo Engineer

Stacie Shaw
Benthic Geo Engineer

Zaid Bahari
Benthic Geo Tech

Cid Dieguez
Benthic Geo Tech

Andre Melo
Benthic Geo Tech

Hafiz Zulkag
Benthic Geo Tech

MMA survey

Kyle Foster
MMA Survey Engineer

Matthew Long
MMA Survey PC

William Smith
MMA Survey Engineer

Virginie Ugo
MMA Surveyor

MMA Valour crew

Akhmad Damora
Master

Mustofa Lutfi
Master

Fadrizal Bin Mahmad Subri
Chief Engineer

Cheah Phi Shin
Chief Engineer

Lania Kurniauan
Chief Officer

Mohd Jaya Aqua
Chief Officer

Wendy Padda
Chief Officer

Yuspina Palayukan Pasiang
Chief Officer

Comia June Madlangbayan
Second Officer

Ritzy Lopez
Second Officer

Rio Nevanda Satria Pratama
Second Officer

Danang Prayogi

Second Officer

Estoce Amador Evans
ETO

Wan Mohd
ETO

Asfie Eka
Second Engineer

Adwin Ponuraj
Second Engineer

Jeffrey Dizon Tan
Third Engineer

Burhanuddin Bin Muhammad
Bosun

Raiyaz Ahmed Mohammed
Cook

Abu Sukur
Cook

Yadav Sunil
Cook

Marc Anthony Jr Alxala Maduro
Steward

Mharlou Ano
Steward

Ashwin Pareechuvalappil
Steward

Gelayan Rawing
Steward

Muhammad Sayuti
Steward

Dennis Churchill
AB

Gowtham Gopalakrishnan
AB

Evangelista Ricardo Jr
AB

Wayne Oto Hutchinson
Fitter

Gimeno Erwin Divinagracia
Oiler

Bremen Core Repository, MARUM, University of Bremen

Leonie Everding
Temporary student assistant

Frederick Hardeel
Temporary student assistant

Ronja Kuhnlein
Temporary student assistant

Nielle Lacson
Temporary student assistant

Leola Pfaffling
Temporary student assistant

Jana Steffen
Temporary student assistant

Carolina Teixera de Melo
Temporary student assistant

Javiera Urdangarin Mahn
Temporary student assistant

Abstract

Our understanding of the mechanisms controlling eustatic sea level and global climate changes has been hampered by a lack of appropriate fossil coral records over the last 500 ky, particularly into and out of the glacial periods. This problem was addressed by International Ocean Discovery Program Expedition 389 by drilling a unique succession of Hawaiian drowned coral reefs now at 110–1300 meters below sea level (mbsl). The four objectives are to investigate (1) the timing, rate, and amplitude of sea level variability to examine cryosphere and geophysical processes, including the assessment of abrupt sea level change events; (2) the processes that determine changes in mean and high-frequency (seasonal–interannual) climate variability from times with different boundary conditions (e.g., ice sheet size, $p\mathrm{CO_2}$, and solar forcing); (3) the response of coral reef systems to abrupt sea level and climate changes; and (4) the variation through space and time of the subsidence and the volcanic evolution of the island. To achieve these objectives, 35 holes at 16 sites ranging 131.9–1241.8 mbsl were drilled during the expedition. A total of 425 m of core was recovered, comprising reef (83%) and volcanic (17%) material. Average core recoveries were 66%, with numerous intervals characterized by very well preserved mixtures of coralgal and microbialite frameworks with recoveries >90%. Some science-critical shallow sites were not drilled due to a failure to secure permits to operate in Hawaiian state waters. Furthermore, apart from one site the target penetration depths were not achieved. Preliminary radiometric dates indicate that the recovered reef deposits are from 488 to 13 ka in age. The Onshore Science Party took place in February 2024. Cores were CT and hyperspectral scanned and described. Standard measurements were made, and samples were taken for postcruise research. Preliminary assessment of the age and quality of the reef and basalt cores suggest that many of the expedition objectives will be met.

Plain language summary

Shallow marine corals are highly sensitive to sea level and global climate change and preserve a reliable record of past sea level and climate conditions. Knowledge of sea level and global climate variations over the past half a million years is severely limited because of a lack of continuous fossil coral records over this time. To address the critical need for coral records, this project focuses on the submerged fossil reefs around the island of Hawai'i. Frequent and large volcanic eruptions formed and continue to grow the island of Hawai'i, and the island and surrounding shallow coral reefs are pushed down at a rapid and nearly constant rate because of the weight of the volcanic rock erupted onto the land. As the land and coral reefs subside, coral reef growth can match the subsidence rate, and changes in sea level and global climate are preserved in a unique and near-continuous fossil coral record covering the last half a million years. Scientific drilling of these reefs will provide a new record of climate and sea level change, including several key time periods where sea level and climate conditions are poorly known. The project has four major scientific objectives: (1) to measure the extent of sea level change over the past half a million years, (2) to investigate why sea level and climate change through time, (3) to investigate how coral reefs respond to abrupt sea level and climate changes, and (4) to improve scientific knowledge of the growth and subsidence of Hawai'i over time. Expedition 389 drilled 35 holes at 16 sites ranging from 131.9 to 1241.8 meters below sea level, recovering 425 meters of core, including very well-preserved mixtures of coralgal and microbialite reef frameworks as well as interlayered and basement volcanic rocks. Preliminary observations and radiometric data confirm that these deposits span the past ~500,000 years, including numerous key periods of major global ice sheet and sea level instability.

1. Introduction

Drowned coral reefs on rapidly subsiding margins (e.g., Hawai'i [USA] and Papua New Guinea) contain a unique and largely unexploited archive of sea level and climate changes (Webster et al., 2007, 2009; Hibbert et al., 2016). Depending on the relationship between eustatic sea level changes and reef growth, the rapid subsidence ensures that these settings have the unique potential to continually create accommodation space, thus generating greatly expanded stratigraphic sections compared to reefs from stable and uplifting margins (Figure **F1a**). Moreover, these drowned reefs

evolved mainly during different periods of Earth's sea level and climate cycles (i.e., glacial periods) that are not well sampled by reefs at stable and uplifting margins (Woodroffe and Webster, 2014). Our understanding of the mechanisms that control abrupt climate change and eustatic and regional sea level change is significantly hampered by a lack of appropriate fossil coral records over the last 500 ky, particularly during the transitions into, during, and out of the glacial periods (Lambeck et al., 2002). Crucial new coral reef data are needed to directly constrain the timing, rate, and amplitude of sea level variability during not only the last glacial cycle, where the data are still controversial (e.g., Woodroffe and Webster, 2014; Yokoyama et al., 2018, 2022), but also over the last 500 ky. Such data will address climatic and cryospheric processes and assess controversial abrupt sea level events (i.e., meltwater pulses) that occur on suborbital frequencies (Chappell, 2002; Thompson and Goldstein, 2005; Yokoyama et al., 2001). Identification of the factors and processes that control annual average global climate and seasonal and interannual climate variability in the subtropical Pacific is of equal importance. Theories of how regional oceanography and hydroclimate respond to external forcing and/or are a result of internal sources of variability are primarily derived from models or analyses of instrumental records and are generally limited to the last century, when only small changes in mean climate occurred (e.g., Dai et al., 2015; Kavanaugh et al., 2018). Earth history over the last 500 ky reveals that the "dynamic range" of climate change is much larger than in the instrumental record and that high-frequency global and regional climate sensitivity to external forcing is dependent on mean state (Köhler et al., 2018). Prime tests of these theories require paleoclimate records (particularly seasonal-resolved fossil coral archives) from times when climate forcing, such as pCO_2 and solar insolation, were different than today.
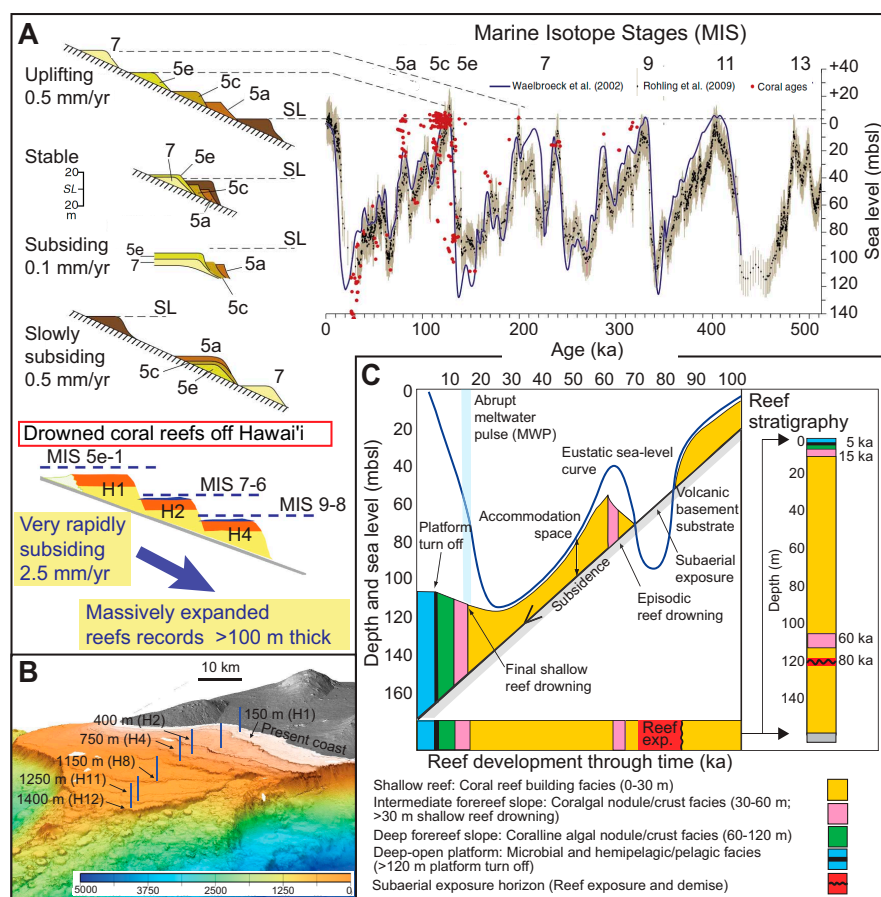

Figure F1. A. Response of coral reefs to sea level change in different tectonic settings, with continuous preserved sea level records and reliably dated corals (red dots) over the past 500 ky (after Woodroffe and Webster, 2014). B. Bathymetric map of the Kawaihae and Mahukona terraces resulting from subsidence and sea level change. Data from MBARI Mapping Team (2000) and Smith et al. (2002). Image created by Jenny Paduan, MBARI. C. Conceptual model showing the relationship between reef growth, sea level changes, and subsidence that allows Expedition 389 scientists to reconstruct a globally unique record of sea level, climate, and reef growth over the past 500,000 y (after Webster et al., 2007, 2009).

2. Background

2.1. Hawaiian reefs

The Hawaiian fossil coral reefs grew and drowned episodically over the last 500 ky and offer a unique opportunity to address major scientific problems. Hawai'i represents the ideal study location for three main reasons (Webster et al., 2009). First, there is rapid subsidence due to flexure of the oceanic lithosphere from loading of the growing volcanoes, which in turn is controlled by rheology of the lithosphere and mantle (Watts, 1978); this process creates accommodation space that results in expanded reef sections, in contrast to convergent margins (e.g., Barbados and Papua New Guinea) and passive margins (e.g., the Great Barrier Reef), where most existing fossil reef records are derived (Figure **F1a**). Short-term fluctuations in volcanic loading are averaged out, and thus subsidence rate is nearly uniform at 2.5–2.6 m/ky over tens to hundreds of thousands of years (Webster et al., 2009; Puga-Bernabéu et al., 2016). The depths of the sequence of drowned reefs off shore Hawai'i (Figure **F1b**) fits the timing of the last six interglacials only if the subsidence rate remained nearly constant for the last 500 ky. Second, Hawai'i is uniquely situated; it is well away from the confounding influence of large ice sheets and boundary ocean currents that might obscure the sea level, and it fills a large geographical data gap because the abyssal seafloor in the subtropical Pacific Ocean is generally too deep to preserve carbonate-rich sediment for subtropical climate variability reconstructions. Third, an extensive database of bathymetry, submersible and remotely operated vehicle (ROV) observations, and sedimentary and radiometric data confirm that the drowned reefs are highly sensitive to abrupt changes in sea level and climate. This wealth of site survey information was used to plan Expedition 389 operations.

2.2. Conceptual and numerical model of reef evolution in response to rapid subsidence

The relationships between reef initiation, subsidence of the basement, eustatic sea level changes, and reef growth during changes in accommodation space can be modeled (Figure **F1c**). Previous work on Hawai'i (Ludwig et al., 1991; Moore and Fornari, 1984) and Papua New Guinea (Galewsky et al., 1996; Webster et al., 2004b, 2004c) proposed that reef growth initiates during stable sea level highstands and continues throughout the regression, with final drowning during the early part of the deglaciations, perhaps because of abrupt eustatic sea level rise associated with meltwater pulse events (Webster et al., 2004a; Sanborn et al., 2017). Depending on the rate and magnitude of these parameters and reef response, the reef experiences repeated periods of shallow and deep water accretion, brief subaerial exposure, and drowning events, forming a complex "layer cake" stratigraphic succession composed of shallow to deep reef packages, separated by subaerial exposure horizons and drowning unconformities. As a direct result of Hawai'i's rapid but nearly constant subsidence, a thick (100–150 m) expanded sequence of shallow coral reef–dominated facies should be preserved in the Hawaiian reefs that are either unrepresented or a highly condensed sequence on stable (e.g., Great Barrier Reef [Webster and Davies, 2003; Humblet and Webster, 2017]) and uplifted margins (e.g., Papua New Guinea [Lambeck and Chappell, 2001] and Barbados [Schellmann and Radtke, 2004]) because of a lack of continual creation of accommodation space and unfavorable shelf morphology (Woodroffe and Webster 2014). Webster et al. (2007) combined observational data and numerical modeling techniques to simulate the stratigraphic evolution of the two shallowest Hawaiian drowned reefs (H1 and H2), showing that although experiencing subaerial exposure, the interior coral reef deposits (i.e., those deposits retrieved by drilling) are less likely to be diagenetically altered when compared with their stable and uplifted fossil reef counterparts given the brevity (<5 ky) of each subaerial exposure event. The data also suggests that the final reef units, marking the final drowning, were unlikely to be subaerially exposed given the rate of subsidence and eustatic sea level rise during the penultimate and last deglaciations (Webster et al., 2004a; Sanborn et al., 2017). Therefore, reef material recovered from the reef interior, and certainly the last phase of growth, should yield precise radiometric ages and geochemical climate proxies providing critical information about the timing, rate, and amplitude of eustatic sea level changes and associated climate variability of the two last glacial periods (Webster et al., 2009) and based on site survey data, the last five or six glacial periods (Figure **F2**).

2.3. Reef terraces: distribution, morphology, and age data

Based on compiled bathymetric data sets (Figure **F3**) (from MBARI Mapping Team [2000] and Smith et al. [2002]), we identified 13 major (designated H0–H12 from shallowest to deepest [H is for Hawai'i]) and 9 minor reef terraces (designated with suffixes a, b, c, etc.) around Hawai'i and
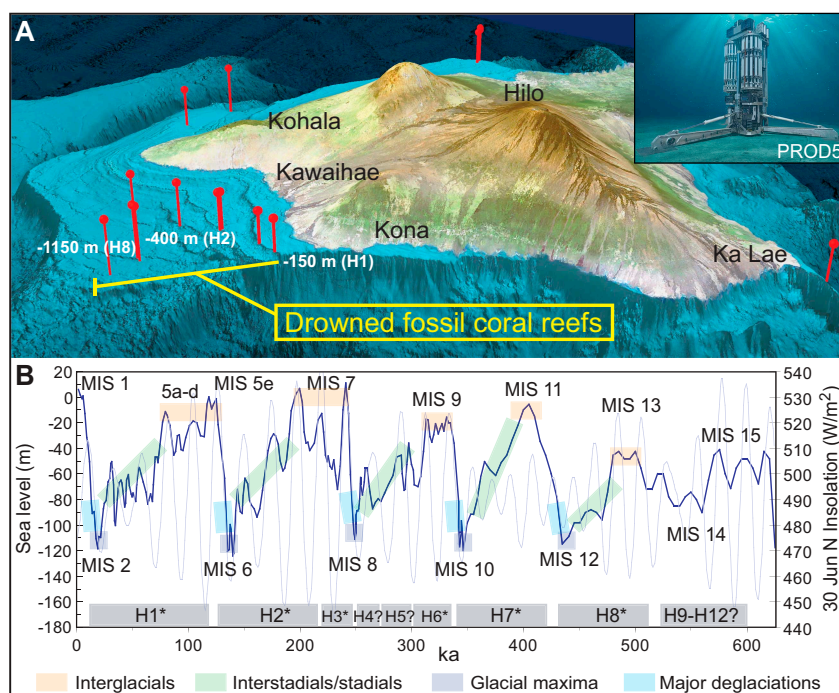

Figure F2. A. Globally unique sequence of drowned fossil coral reefs (H1–H12) off Hawai'i that were proposed to be drilled (red markers) during Expedition 389. Inset: artistic representation of the PROD5 seafloor drill. B. Sea level, climate, and insolation history over the last 600 ky (Imbrie et al., 1984; Berger and Loutre, 1991; Lea et al., 2002). Observational and numerical modeling data indicate the Hawaiian reefs (H1–H12) span each interglacial, interstadial/stadial, glacial maxima, and deglacial interval over the past 500-600,000 y (Webster et al., 2009).

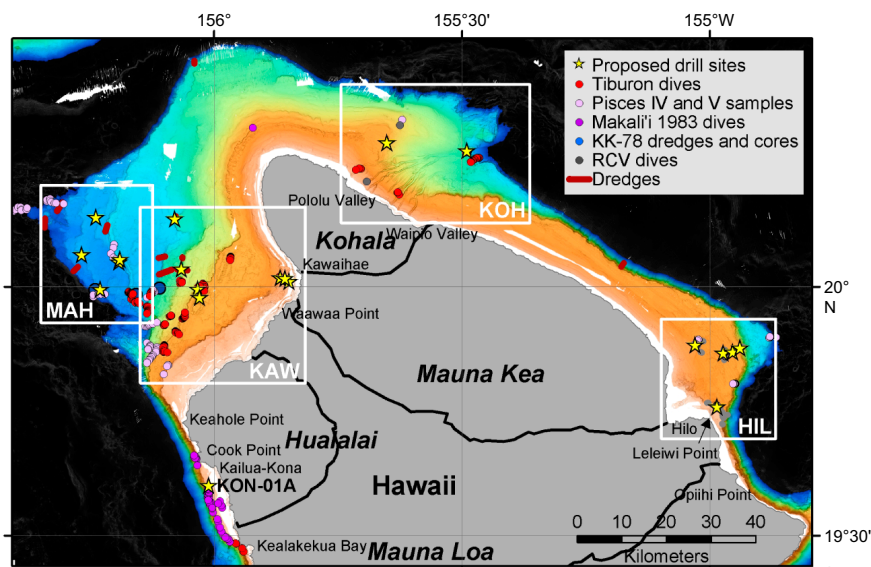**Figure F3.** Map showing proposed Expedition 389 drill sites (yellow stars) and available site survey data sets (high-resolution bathymetry, backscatter, dredge, submersible, and ROV dive observations and samples) for drowned reef terraces. Boxes = locations of close ups (Figure F7) showing details of originally proposed drill sites (data from MBARI Mapping Team [2000] and Smith et al. [2002]; image created by Jenny Paduan, MBARI).

initially selected 11 primary and 9 alternate drilling targets (Figures **F4**, **F5**, **F6**, **F7**). In many cases, the depth of the break-in-slope of a continuous terrace varies because of variable subsidence that produces tilting and secondary retreat due to erosional processes. Detailed summaries of the published reef terrace distribution, morphology, and age data are found in the following studies: Webster et al. (2009), Puga-Bernabéu et al. (2016), Sanborn et al. (2017), and Taylor (2019). Here we provide a summary of the site survey data and site selection process.

Figure F4. Map of the Kawaihae region showing drowned reefs H1–H6, Expedition 389 proposed drill sites (KAW-01A through KAW-07A), and available site survey data (from MBARI Mapping Team [2000] and Smith et al. [2002]; image created by Jenny Paduan, MBARI).
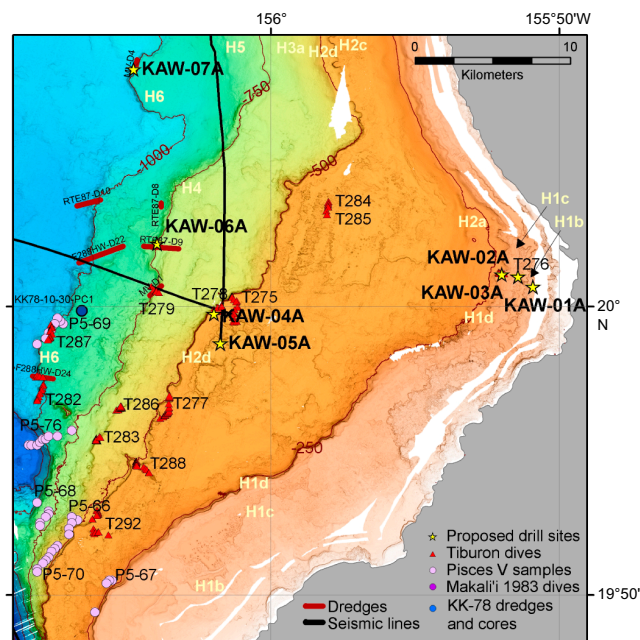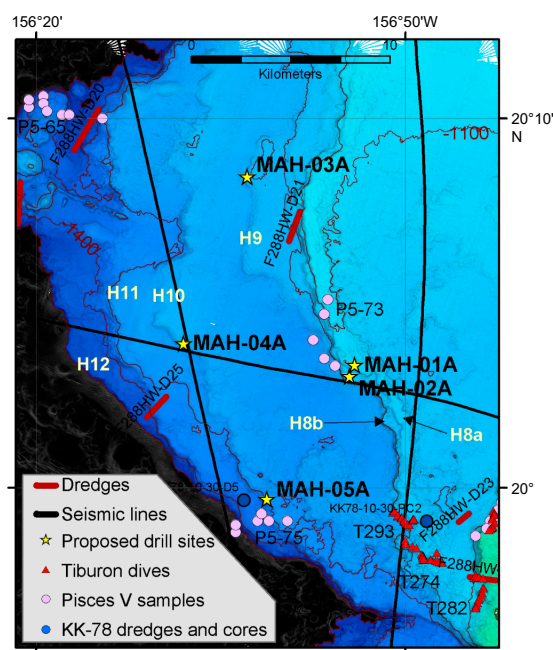

Figure F5. Map of the Mahukona region showing drowned reefs H8–H12, Expedition 389 proposed drill sites (MAH-01 through MAH-5A), and available site survey data (from MBARI Mapping Team [2000] and Smith et al. [2002]; image created by Jenny Paduan, MBARI).

2.4. Site survey data

The assembled site survey data set used to select the drilling sites represents work by many institutions and researchers over the last 40 y. High-resolution swath bathymetry and backscatter, in combination with ROV/submersible and dredge data from proposed drilling locations or adjacent locations, were the primary data sets used to define the extent and characteristics of the fossil reefs and select the proposed drill sites (Figures **F4**, **F5**, **F6**, **F7**; see the Scientific Prospectus [Webster et al., 2023]). Swath bathymetric data were collected in 1998 with a 30 kHz Simrad EM300 system by

Figure F6. Map of the Hilo region showing drowned reefs H1–H7, Expedition 389 proposed drill sites (HIL-01A through HIL-05A), and available site survey data, including example of high-resolution backscatter data available for proposed drill sites. Drowned reefs are characterized by distinct, high (white) backscatter signatures (data from MBARI Mapping Team, 2000 and Smith et al., 2002, image created by Jenny Paduan, MBARI; also published in Puga-Bernabéu et al. [2016]).
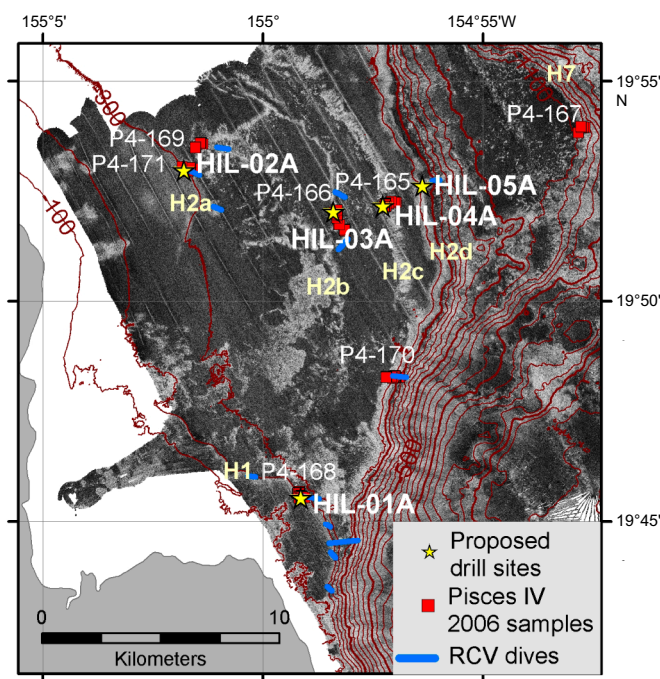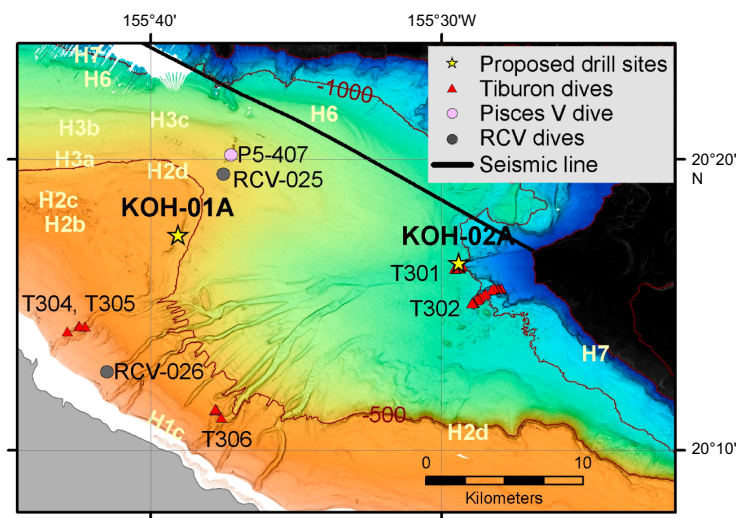

Figure F7. Map of the Kohala region showing drowned reefs H2–H7, Expedition 389 proposed drill sites (KOH-01A and KOH-02A), and available site survey data (from MBARI Mapping Team [2000] and Smith et al. [2002]; image created by Jenny Paduan, MBARI).

the Monterey Bay Aquarium Research Institute (MBARI) on the Kohala Terrace (named by Campbell, 1986) and the northeast margin of Kohala Volcano (Clague et al., 1998; MBARI Mapping Team, 2000) and by the United States Geological Survey (USGS) offshore Hilo (Dartnell and Gardner, 1999). These data are much higher resolution and have superior navigation to all previous surveys, and they form the primary data used for site selection. In addition to the new 30 kHz data, Sea-Beam swath bathymetry was collected during a series of cruises by the Japan Agency for Marine-Earth Science and Technology (JAMSTEC) starting in 1998 (Smith et al., 2002). Additional swath data has been collected by the University of Hawai'i and the National Oceanic and Atmospheric Administration (NOAA) Mapping Group. All data were used to define the extent and characteristics of the reefs and select drill sites. Several air gun lines crossing the terraces were collected during the GLORIA surveys (USGS Cruise F6-86-HW) in 1986.

A great deal of work has already been done to sample and observe the reefs around Hawai'i, starting in 1983 with *Makali'i* submersible dives (M288–M298) (Figure **F5**), mainly on Reef H1d but also one dive on Reef H2c off Kohala (Dive M287) (Figure **F7**). In 1985, *Pisces V* submersible dives (P5-65 through P5-78) explored and sampled many of the reefs off the Kona coast. Dredging programs were undertaken from the R/V *Melville* in 1987 (RTE87-D7 through RTE87-D9) and 2005 (TUIM-MV-D1 through TUIM-MV-D4) and from the R/V *Farnella* in 1988 (F2-88-HW-D18 through F2-88-HW- D25) and 1991 (F2-91-HW-D2) on the northeast Reef H2d on Mauna Kea. One additional *Pisces V* dive (P5-407) and two ROV dives (RCV25 and RCV26) in 1999 took place on the terraces east of Kohala (Figure **F7**). A total of 7 *Pisces IV* dives (P4-165 through P5-171) and video transects during 13 *RCV-150 ROV* dives (RCV334–RCV346) were conducted on the reefs offshore Hilo (Figure **F6**). The Hawai'i Undersea Research Laboratory has also conducted at least 100 additional submersible dives and ROV video transects on these reefs for fishery and other biological studies. In total, over 550 samples of reef carbonate collected during these operations have been examined.

In 2001, MBARI's ROV *Tiburon* completed 14 dives on the reefs southwest of Kohala (T275–T279, T282–TT288, and T291–T293) and 5 dives on the reefs and canyons east of Kohala (T301, T302, and T304–T306) (Figure **F7**). One of these dives (T301) provided observations of a reef interior stratigraphy that represents reef initiation, growth, and drowning. At this location, ROV sampling at the base and top of this exposed section, combined with detailed observations, reveals at least six distinct reef units. These are characterized by different in situ coral volumes and framework types that are separated in places by planar surfaces, perhaps representing either thick coralline algal crusts and/or subaerial exposure surfaces. U-series dating of two coral samples from near the base of this reef yield ages of 377–392 ka (Webster et al., 2009), indicating this reef likely grew during Marine Isotope Stages (MISs) 10 and 11 (Figure **F8**).
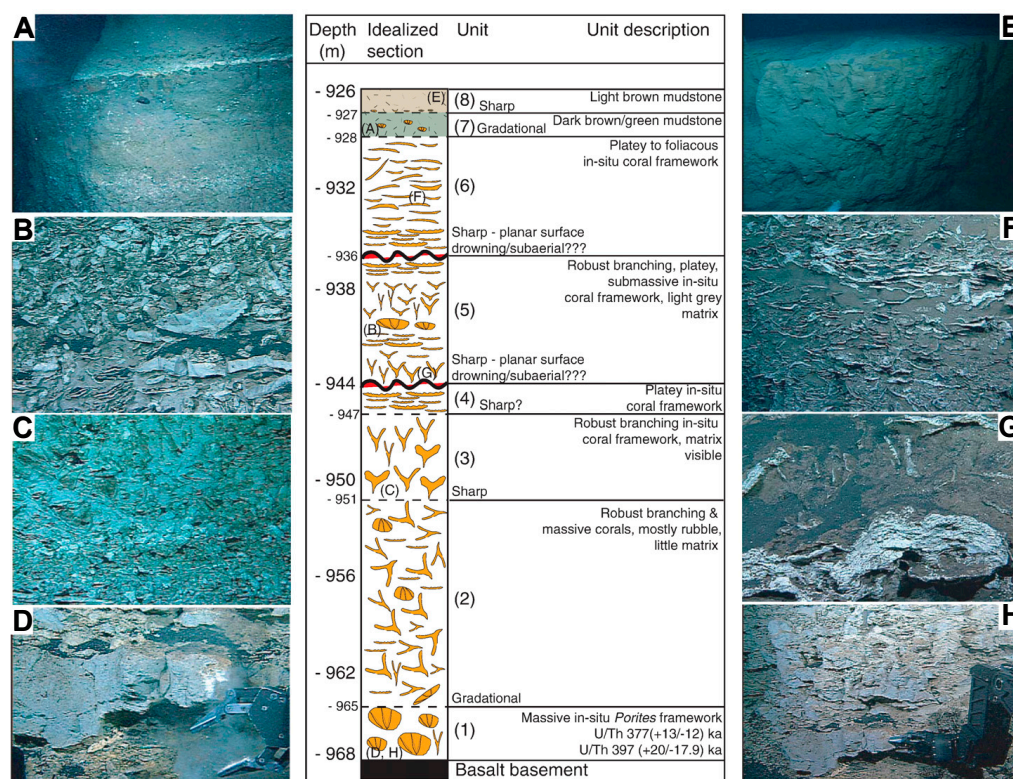
Figure F8. Stratigraphic section through drowned Reef H7 (−950 m) off Kohala, northeast Hawai'i, and outcrop images. A. Transition from Unit 6 to Unit 8. Note sharp contact defined by carbonate? debris between Units 7 and 8. B. In situ platey and submassive coral framework from Unit 5. C. Transition from Unit 2 to Unit 3 characterized by coral rubble and in situ robust branching coral framework respectively. D, H. Unit 1 dominated by in situ massive *Porites lobata*? forming shallow coral reef facies. U/Th age data indicate unit was deposited during MIS 11 (377–397 ka). E. Light brown hemipelagic mudstone forming Unit 8 at top of section. F. In situ platey to foliaceous coral framework toward top of Unit 6. Unit is characterized by thin overlapping agaricid corals (*Leptoseris* and *Pavona*) with intergrowing coralline algae (i.e., *Lithothamnion prolifer*) representing intermediate, fore-reef slope facies. G. Sharp planar surface separating Units 4 and 5 (after Webster et al., 2009).

3. Scientific objectives

The scientific objectives for Expedition 389 directly address key International Ocean Discovery Program (IODP) strategic objectives to investigate the mechanisms that control rapid climate change and the relationship between changes in mean climate state and high-frequency (seasonal–decadal) climate variability. Specifically, it is directly aligned with the Earth's Climate System, Feedbacks in the Earth System, and Tipping Points in Earth's History Objectives of the 2050 Science Framework of IODP. The specific objectives of the project are as follows.

3.1. Objective 1: to define the nature of sea level change in the central Pacific over the last 500 ky

We aim to reconstruct the most complete and detailed sea level record from fossil corals, particularly into, during, and out of the glacial periods. These data will allow more detailed testing of the sensitivity and vulnerability of ice sheet responses to orbital to millennial-scale climate change. A sea level curve will be built using absolute radiometric dating methods (^{14}C accelerator mass spectrometry [AMS] <50 ka and U/Th) of in situ corals and coralline algae, paleobathymetric data, and published and directly calculated subsidence rates for Hawai'i.

3.2. Objective 2: to reconstruct paleoclimate variability for the last 500 ky and establish the relationship between the mean climate state and seasonal–interannual variability

We aim to use coral-derived temperature and precipitation records to investigate how high-latitude climate (e.g., ice sheet size), atmospheric CO_2 levels, and mean and seasonal solar radiation impact Hawaiian climate, including storminess and the position of the Intertropical Convergence Zone. In combination with theoretical studies of subtropical climate change, these records will allow for the identification and study of critical processes that determine Pacific-wide climate.

3.3. Objective 3: to establish the geologic and biological response of coral reef systems to abrupt sea level and climate changes

We aim to reconstruct the detailed stratigraphic, geomorphic, and paleoenvironmental evolution of each reef in response to abrupt sea level and climate changes; test ecological theories about coral reef resilience and vulnerability to past and future climate changes by assessing the nature and rate of change in reef communities within and between successive reefs over interglacial–millennial timescales; and establish the nature of living and ancient microbial communities in the reefs and their role in reef building.

3.4. Objective 4: to elucidate the subsidence and volcanic history of Hawai'i

We aim to refine the variation through space and time of the subsidence of Hawai'i and contribute to understanding the volcanic evolution of the island. The key to these objectives is to obtain well-dated volcanic samples from the base of each hole and interbedded within or draping over the reefs.

4. Operational strategy

4.1. Site selection and locations

A total of 11 primary sites and 9 alternate sites were originally selected (Figures **F3**, **F4**, **F5**, **F6**, **F7**), located in water depths ranging approximately 129–1234 meters below sea level (mbsl) with maximum penetration depths of ≤110 meters below seafloor (mbsf). Although most of the original primary and some alternate sites were drilled during Expedition 389, the site selection and drilling strategy changed after the expedition was underway because of three main factors. First, PROD5, the seabed drilling system, was unable to reach the planned penetration depths at all but one site. Thus, the strategy was adjusted to drill more shallow penetration holes (20–40 mbsf) at several sites, and, additionally, IODP Environmental Protection and Safety Panel (EPSP) and European Consortium for Ocean Research Drilling (ECORD) Facility Board (EFB) approval was obtained to drill a new site during the expedition (Site M0107). Second, because Expedition 389 was unable to secure permission to operate in state waters, the three primary science-critical sites (in the Kawaihae, Kona, and Hilo regions) located on the H1 terrace could not be drilled; as a consequence, IODP panel approval was also obtained during the expedition to drill new sites (M0099, M0106, and M0110) on the H1 terrace not in state waters, even though they are not ideally located to meet some important scientific objectives. Third, based on observations of reef material recovered early during the expedition at Site M0097, it appeared that moving drill sites closer to the seaward edge of the terrace would result in recovery of more submassive and massive fossil corals. Although the 150 m radius of each site target allowed for this flexibility at most sites, this was not the case at proposed Site MAH-02A (Figure **F7**); thus, IODP panel approval was obtained during the expedition to drill a new site (M0108), located on the same terrace ~200 m south of Site MAH-02A. IODP Expedition 389 sites (Figure **F9**; Table **T1**) are distributed across five regions around the island of Hawai'i: Kawaihae (Figure **F10**), Mahukona (Figure **F11**), Kohala (Figure **F12**), Hilo (Figure **F13**), and Ka Lae (Figure **F14**).
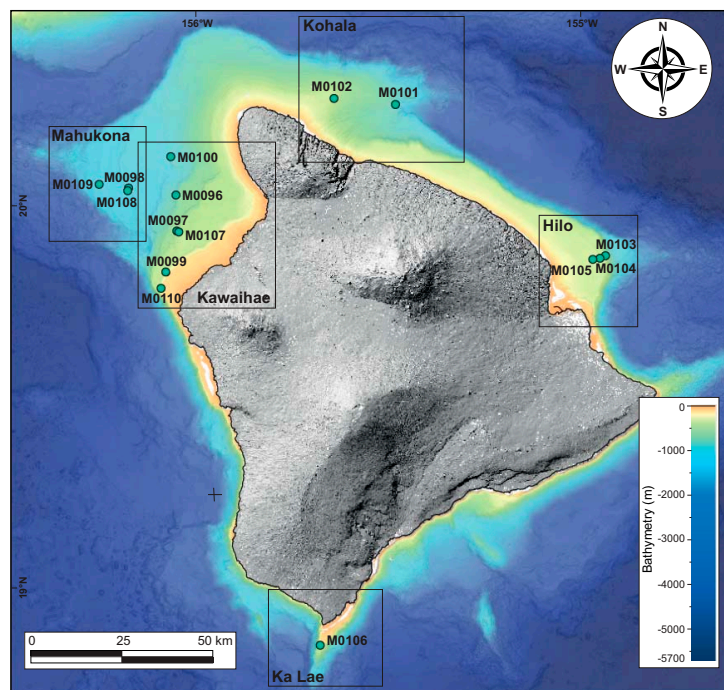
Figure F9. Expedition 389 final site locations from the five regions overlaid on the 50 m bathymetric map offshore Hawai'i (SOEST, 2016; **https://www.soest.hawaii.edu/hmrg/multibeam/grids.php#50mBathy**).

Table T1. Hole summary, Expedition 389. R = rotary coring mode, W = wash down mode, P = push coring mode.

| Hole	Latitude (WGS84)	Longitude (WGS84)	Coring method	Water depth (m)	Total drilled depth	Recovered length (m)	Recovery (%)	Total cores (N)	Date started (2023)	Date finished (2023)
389-										
M0096A	20.036388°	−156.065720°	R	740.8	1.78	1.62	91	2	5 Sep	5 Sep
M0096B	20.036439°	−156.065665°	W	739.1	0.99	0.00	0	1	6 Sep	6 Sep
M0096C	20.036423°	−156.065688°	R; W	739.9	1.74	0.45	52	1	6 Sep	6 Sep
M0096D	20.036843°	−156.065610°	R	736.8	7.40	2.24	30	4	7 Sep	7 Sep
M0096E	20.036980°	−156.065609°	W	738.2	6.70	0.00	0	0	19 Sep	19 Sep
M0096F	20.036960°	−156.065596°	W; R	738.2	12.24	4.76	86	5	20 Sep	20 Sep
M0097A	19.942137°	−156.062853°	R	414.2	35.05	26.42	75	25	7 Sep	9 Sep
M0097B	19.942109°	−156.062877°	R; W	414.6	59.35	23.17	93	12	10 Sep	12 Sep
M0097C	19.942525°	−156.063655°	R	417.6	36.16	28.04	79	32	15 Sep	18 Sep
M0097D	19.942699°	−156.063477°	R	424.0	23.69	19.22	81	28	30 Oct	31 Oct
M0098A	20.055425°	−156.189735°	R; W	1100.1	19.10	8.42	45	23	13 Sep	15 Sep
M0099A	19.834423°	−156.091288°	R	131.9	6.44	4.29	67	6	21 Sep	21 Sep
M0099B	19.834342°	−156.091199°	R	131.9	6.40	4.35	68	5	21 Sep	22 Sep
M0099C	19.834348°	−156.091261°	R	131.9	38.31	25.50	67	27	22 Sep	23 Sep
M0099D	19.834411°	−156.091324°	W	131.7	27.71	0.00	0	0	24 Sep	24 Sep
M0099E	19.835240°	−156.092441°	R	144.6	31.62	18.00	57	25	26 Sep	27 Sep
M0099F	19.835338°	−156.092304°	R	145.6	13.45	6.75	50	9	26 Sep	27 Sep
M0099G	19.835295°	−156.092467°	W; R	146.3	68.62	18.93	49	31	19 Oct	23 Oct
M0100A	20.137606°	−156.079107°	R	998.0	12.43	9.73	78	12	30 Sep	1 Oct
M0101A	20.273677°	−155.489903°	P; R	931.9	18.09	12.34	68	29	2 Oct	3 Oct
M0101B	20.273832°	−155.489799°	R	932.0	45.15	26.44	93	27	5 Oct	7 Oct
M0102A	20.289982°	−155.650868°	R	412.8	25.14	11.08	44	14	4 Oct	4 Oct
M0102B	20.289949°	−155.650948°	W	415.4	4.70	0.00	0	0	8 Oct	8 Oct
M0102C	20.289871°	−155.651009°	W; R	415.9	73.44	42.32	79	33	8 Oct	11 Oct
M0103A	19.877010°	−154.939609°	R	404.5	45.61	14.31	31	33	11 Oct	14 Oct
M0104A	19.870311°	−154.954000°	R	347.0	46.39	42.99	93	22	14 Oct	16 Oct
M0105A	19.867494°	−154.972719°	R	339.5	26.08	7.63	29	14	16 Oct	17 Oct
M0106A	18.856679°	−155.688330°	R	148.6	7.43	1.47	20	4	17 Oct	18 Oct
M0106B	18.856772°	−155.688265°	R	147.9	16.14	2.98	32	10	18 Oct	19 Oct
M0107A	19.940185°	−156.058178°	R	403.8	13.44	12.72	95	8	23 Oct	24 Oct
M0108A	20.048364°	−156.192745°	R	1178.1	1.97	1.95	99	6	24 Oct	24 Oct
M0108B	20.048346°	−156.192127°	W; R	1177.2	30.70	16.35	63	33	24 Oct	26 Oct
M0109A	20.065169°	−156.266938°	R	1241.8	4.62	4.21	91	12	27 Oct	27 Oct
M0110A	19.793231°	−156.105784°	R	156.9	18.70	14.18	76	18	28 Oct	29 Oct
M0110B	19.792508°	−156.104756°	R	144.8	17.22	12.90	75	10	29 Oct	30 Oct
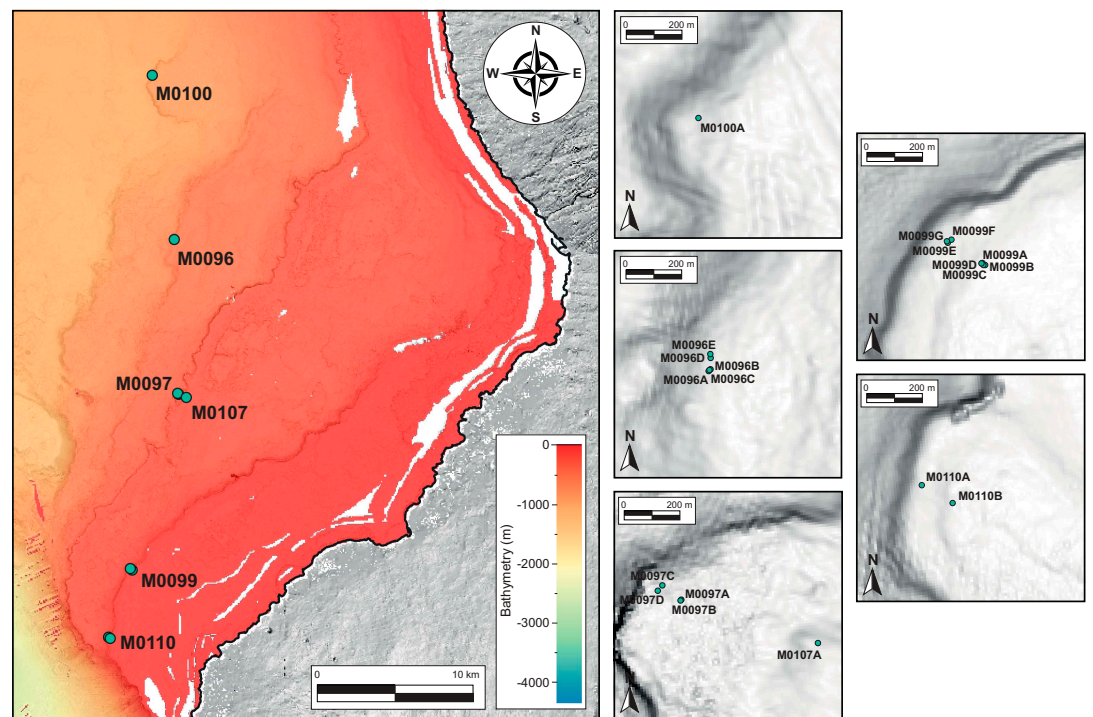
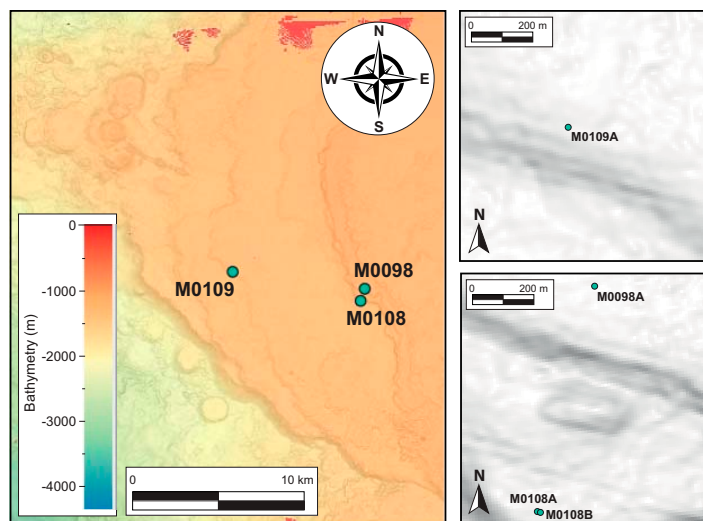**Figure F10.** Kawaihae region site locations for Sites M0096, M0097, M0099, M0100, M0107, and M0110 overlain on a 10 m grid bathymetric map (**https://www.ncei.noaa.gov/maps/bathymetry**).

Figure F11. Mahukona region site locations for Sites M0098, M0108, and M0109 overlain on a 10 m grid bathymetric map (**https://www.ncei.noaa.gov/maps/bathymetry**).
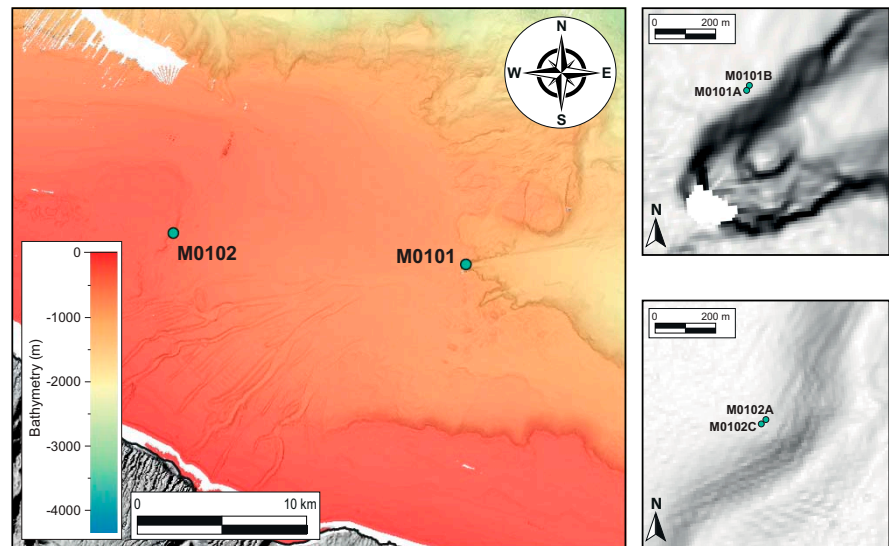
Figure F12. Kohala region site locations (Sites M0101 and M0102) overlain on a 10 m grid bathymetric map (**https://www.ncei.noaa.gov/maps/bathymetry**).
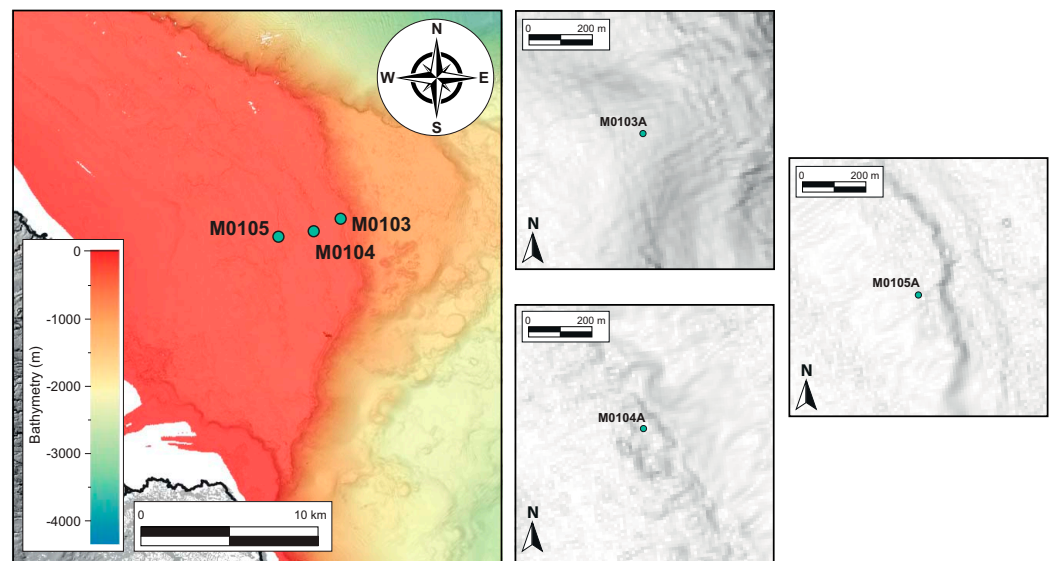
Figure F13. Hilo region site locations for Sites M0103–M0105 overlain on a 10 m grid bathymetric map (**https://www.ncei.noaa.gov/maps/bathymetry**).
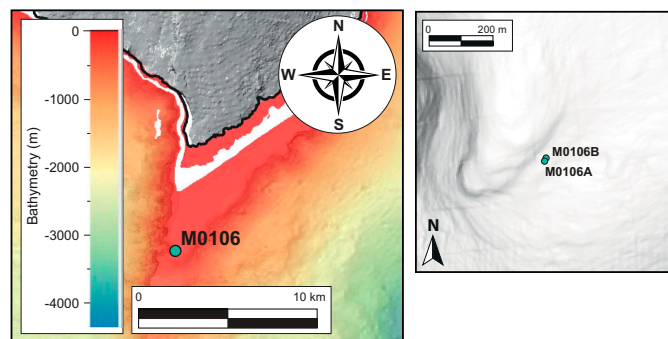
Figure F14. Ka Lae region location for Site M0106 overlain on a 10 m grid bathymetric map (**https://www.ncei.noaa.gov/maps/bathymetry**).

5. Operations

5.1. Offshore phase

The drilling platform used for Expedition 389 was the dynamically positioned multipurpose vessel *MMA Valour* (84 m long; 4258 tons), operated by MMA Offshore. A suite of containerized laboratories and offices were installed on the aft deck area. Coring operations were performed by Benthic's fifth generation Portable Remotely Operated Drill (PROD) seafloor drill. PROD5 is rated to a water depth of 4000 m, is unaffected by surface heave conditions, and consequently has good control on bit weight, increasing the likelihood of higher quality cores in shallow waters compared to ship-mounted systems that rely on heave compensation.

Rotary coring was the primary drilling method, recovering core with a diameter of 72 mm in 2.75 m sampling barrels. To give some flexibility during rotary coring operations, two different rotary drill bits (diamond surface set and impregnated) were available. One 75 mm diameter push core was attempted at Site M0101, recovering 6 cm of soft sediment in Hole M0101A (Core 389-M0101A-1P-1). A small number of wash bores were usually loaded to allow for advancement without coring or to clean the borehole of material that may have fallen to the bottom during core runs or setting casing. Two core liner types were available: aluminum and polycarbonate.

PROD5 is self-contained with its own Launch and Recovery System (LARS), occupying a basic deck footprint of 17.0 m × 8.0 m and is lowered to the seafloor on an umbilical cable. The computerized control system allows the corer to safely position on the seabed by moving above the sea bed using its onboard thruster and subsea cameras to ensure there are no obstacles and/or significant macro benthos on the selected landing site. Each of PROD5's three legs can be independently adjusted to provide a level platform from which to deploy the core barrels. Upon confirmation of a successful landing on site, the sound velocity profile gathered during deployment to the seafloor was integrated to the ultra-short baseline (USBL) method as part of the process to determine the coordinates of the center of gravity of PROD5. This method takes into account sound velocity error, offset measurement, and pitch and roll corrections. Using the coordinates of the ship as a reference, the latitude and longitude of the hole was calculated with an error of up to 1% of the water depth.

Mobilization of the vessel took place in Barbers Point Harbor, Kapolei, on the island of O'ahu between 26 and 31 August 2023. ECORD Science Operator (ESO) staff boarded on August 26, and the offshore science party participants joined on August 29. The *MMA Valour* set sail at 1750 h on August 31, and the first leg of the offshore phase of the expedition continued to 1000 h on September 27 (Table **T1**), when the *MMA Valour* began transit back to Kapolei, arriving at 0630 h on September 28 for a ~25 h midexpedition port call for a crew and technician change, to load supplies, and to offload the reefer of core collected during Leg 1. The vessel began transit back to site for Leg 2 by 0700 h on September 29 and arrived on location at 0230 h on September 30.

The offshore operational phase of Expedition 389 concluded at 2345 h on October 31 with the transit back to Kapolei for demobilization. The *MMA Valour* arrived at port after 0600 h on November 2, and the offshore scientists disembarked in the early afternoon. The remaining ESO containers and the second refrigerated core reefer containing Leg 2 cores, core catcher samples, and interstitial water splits were offloaded during demobilization for return shipping to final destinations. ESO staff disembarked the vessel on November 4 at the end of Expedition 389 demobilization.

In total, 44.32 days of Expedition 389 were spent operational on station, 1.76 days were spent in transit between sites or from port, 1.0 days were spent in port during the expedition, 14 h were spent on standby at station because of vessel technical issues, 10.94 days were spent on equipment-related downtime, and 2.0 h in a diversion to port for disembarkment of a contractor for medical reasons.

As with the majority of IODP Mission Specific Platform expeditions, no cores were split during the offshore phase; therefore, a comprehensive onshore phase (the Onshore Science Party [OSP])

Table T2. Onshore and offshore measurements, Expedition 389. OSP = Onshore Science Party, IW = interstitial water, ICP-OES = inductively coupled plasma–optical emission spectrometry, IC = ion chromatography, LECO = carbon/sulfur analyzer, XRD = X-ray diffraction.

MMA Valour, offshore Hawai'i	Onshore Science Party, Bremen Core Repository (Germany)
Core description	XCT scanning (pre-OSP)
Geochemistry: pH by ion-specific electrode, alkalinity by single-point titration to pH, salinity by refractometer, ammonium by flow injection method	Core description: split core visual core description and thin section analysis
Whole-core MSCL logging: density, *P*-wave velocity, magnetic susceptibility, electrical resistivity, and natural gamma radiation	Geochemistry IW analysis: ICP-OES (major and trace elements) and IC (chloride, bromide, sulfate, and nitrate), sampling for $\delta^{18}O$
Geochronology	Geochemistry solid phase analysis: TOC/TC by LECO (carbon-sulfur analysis) and XRF bulk element analysis by ED-XRF
Postexpedition microbiological (aDNA) samples for time-sensitive analyses	XRD bulk mineralogy analysis
Smear slide analysis	Discrete sample measurements: moisture and density properties (bulk and grain density and water content porosity), and compressional *P*-wave velocity
	High-resolution continuous digital line scanning of all split-core surfaces
	Thermal conductivity
	Color reflectance and *P*-wave measurements
	Discrete paleomagnetic measurements and discrete magnetic susceptibility measurements
	Hyperspectral imaging

at the IODP Bremen Core Repository (BCR) complemented the offshore phase. Table **T2** summarizes the descriptions and measurements made during Expedition 389 and indicates whether they were conducted offshore or onshore.

5.2. Onshore Science Party

Prior to the OSP, X-ray CT (XCT) scanning for Expedition 389 was conducted on the whole cores at the Core Scanning Facility (CSF) at the British Geological Survey in Keyworth, United Kingdom. The refrigerated core reefers were shipped from Hawai'i to the United Kingdom and were delivered in two shipments to the CSF, arriving on 2 January and 7 February 2024. Following XCT scanning, the core was then shipped to the BCR in four shipments for processing during the OSP, which took place between 6 and 26 February 2024 at the BCR located in the Center for Marine Environmental Sciences (MARUM) building on the campus of Bremen University, Germany. The cores were split and described in detail, and IODP standard sampling and measurements and postexpedition scientific research sampling were undertaken (Table **T2**).

Further analytical laboratories were accessed by agreement with the Department of Geosciences (geochemistry, paleomagnetism, and X-ray diffraction mineralogy) and MARUM (physical properties and nondestructive core logging) at Bremen University (Table **T2**). In addition to the IODP standard suite of analyses performed during the OSP, hyperspectral data were acquired on all archive halves using a SisuROCK drill-core scanner (Spectral Imaging Ltd., Oulu, Finland) to provide information on carbonate mineralogy and diagenetic alteration.

6. Lithologic facies

The combination of the overall lithology, major and minor components, and sedimentary boundaries show the fossil reefs around Hawai'i are composed of thirteen major lithologic facies (Figure **F15**), defined as follows:

- Fall-in material (F0). These deposits are reworked, brecciated material, possibly with recoring marks on some debris at the top of the core, different from the facies below.
- Coralgal boundstone (F1). These deposits are mainly built (bound) by corals and encrusting coralline algae forming well-developed frameworks. Occasional vermetids and *Homotrema* within coralline algal crusts are present.
- Coralgal-microbialite boundstone (F2). These deposits are formed by coral and coralline algae frameworks either capped by microbialites or with large cavities filled by microbialites. Occasional gastropods, echinoid spines, serpulid tubes, bivalves, vermetids, and *Homotrema* are present.
- Microbialite boundstone (F3). These deposits are built mainly by microbialite frameworks with occasional coral and coralline algae crusts.
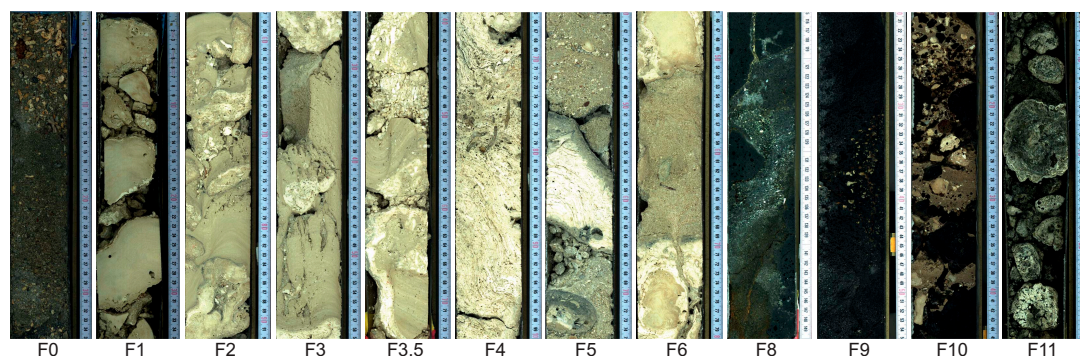
Figure F15. High-resolution line scan images of representative examples of the different lithologic facies observed during Expedition 389.

- Microbialite-algal boundstone (F3.5). These deposits are characterized by a mixture of microbialite and algal boundstones forming well-developed frameworks.
- Algal boundstone (F4). Massive coralline algal crusts forming well-developed frameworks, commonly associated with *Homotrema* and vermetids and with occasional thin corals.
- Consolidated biodetrital (F5). These deposits are biodetrital grainstone or packstone with coral clasts, algal clasts, and various accessory bioclasts (bivalves, gastropods, echinoid spines, and large benthic foraminifers).
- Unconsolidated biodetrital (F6). These deposits are biodetrital carbonate sands with coral clasts, algal clasts, large benthic foraminifers, gastropods, *Halimeda* clasts, and echinoid spines.
- Hemipelagic/pelagic (no image). These mudstone/wackestones and are dominated by planktonic foraminfera, mollusks, small benthic foraminifers, abundant micrite, and minor volcaniclastic grains.
- Volcaniclastic (F8). These deposits are mostly volcaniclastic sediments, with occasional coral clasts as well as large benthic foraminifers.
- Basaltic volcanic rock (F9). This facies is characterized by a diverse suite of massive, vesicular, picritic, and brecciated basaltic rock types.
- Mixed carbonate-volcaniclastic (F10. These deposits are a mixture of consolidated/unconsolidated carbonate-volcaniclastic sediments containing carbonate clasts of corals, algal clasts, *Halimeda* intraclasts, echinoid spines, gastropods, and large benthic foraminifers.
- Rhodoliths rudstone/floatstone (F11). The deposits are either rudstone or floatstones and are dominated by coralline algae forming rhodoliths.

7. Site summaries

7.1. Leeward side

The northwest flank of Hawai'i represents the area of most intensive investigation over the last 40 y. Complete high-resolution bathymetry and backscatter data coverage, combined with extensive ROV and submersible observations and sampling, has revealed a succession of 12 well-developed reef terraces. This area is divided into the proximal drill sites off shore, hereafter referred to as the Kawaihae region (Figure **F10**), and the more distal drill sites off shore the western flank of the submerged Mahukona Volcano (Clague and Moore, 1991; Moore and Clague, 1992), hereafter referred to as the Mahukona region (Figure **F11**).

7.1.1. Kawaihae sites

The original sites on this H1 reef were located in Hawaiian state waters, so they were unavailable for drilling (proposed Sites KAW-01-3B, KON-01A, and HIL-01A). Sites M0099 and M0110 were selected and drilled because they intersect the major 150 mbsl reef terrace (H1d) that can be traced from the originally proposed sites and occur around much of the flanks of the island of Hawai'i (Moore and Fornari, 1984; Webster et al., 2004a). They were drilled at water depths

between 132 and 157 m. ROV observations and samples at these sites confirm their reefal nature. This terrace drowned about 14.7 ka (Webster et al., 2004a; Sanborn et al., 2017) and likely grew during MISs 1–5 (Webster et al., 2009).

The 400 mbsl terrace forms a well-developed and continuous reef (H2d) off Kawaihae. This reef has been extensively sampled and observed by submersible, and U/Th ages on corals range 133 to approximately 170 ka (Webster et al., 2009). A series of holes (414–424 mbsl) were drilled at Site M0097 at the seaward edge of the prominent terrace feature, and Site M0107 was drilled on a shallower subterrace at 404 mbsl. Sites M0096 and M0100 were drilled to recover reefal material from deeper terraces off shore Kawaihae. However, Site M0096, located on the H4 terrace at approximately 740 mbsl, and Site M0100, located on the H6 terrace at approximately 990 mbsl, were only drilled to <15 mbsf and comprise basalt.

7.1.1.1. Site M0096

Site M0096 consists of four holes (M0096A, M0096C, M0096D, and M0096F) located on a terrace at water depths of 736 to 741 m (Figures **F10**, **F16**). The first three holes primarily comprise mixed carbonate-volcaniclastic sediments, bioclastic materials (including corals and coralline algae), and large, subangular to subrounded volcanic clasts of variable crystallinity. In-place basalt was recovered at the base of Hole M0096D. The fourth hole (M0096F) consists entirely of in-place lava flows with variable vesicularity and low crystallinity lava, and lava clinker common in subaerial emplacement conditions.

Multisensor core logger (MSCL) and other MSCL physical properties measurements indicate some variability within the in-place basalt interval, but there are no apparent downhole trends.
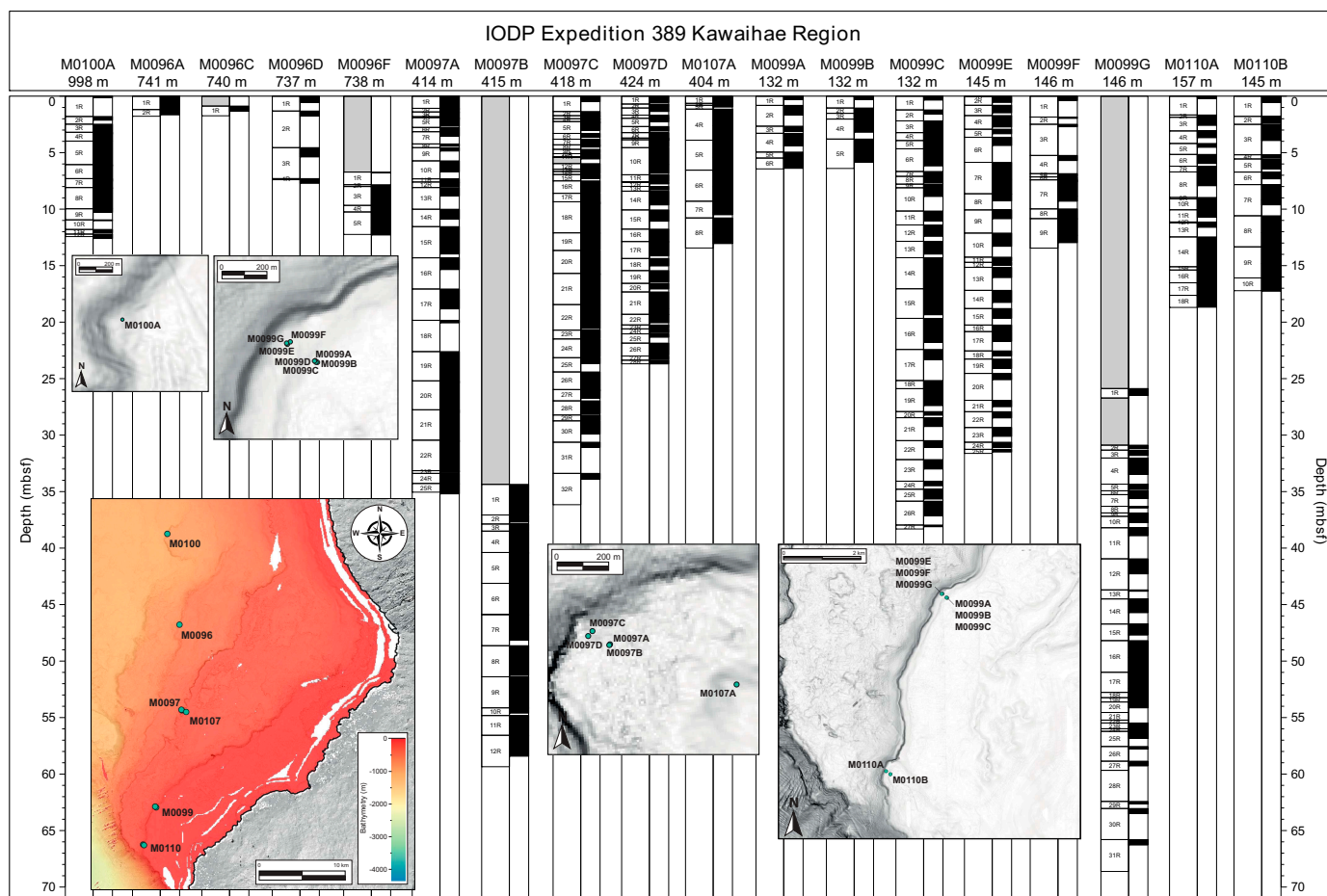

Figure F16. Kawaihae region cores and recovery for Sites M0096, M0097, M0099, M0100, M0107, and M0110, with site location maps overlain on a 10 m grid bathymetric map (**https://www.ncei.noaa.gov/maps/bathymetry**).

One coral near the top of Hole M0096D was dated to 241.4 ± 0.1 ky BP. The date is consistent with the estimated age of the H4 terrace spanning MIS 8/9 (Ludwig et al., 1991; Webster et al., 2009).

7.1.1.2. Site M0097

Site M0097 consists of four holes located on a terrace at water depths of 414 to 424 m. Holes M0097A and M0097B were drilled at a water depth of 414 m, and Holes M0097C and M0097D were drilled closer to the edge of the terrace in slightly deeper water at 424 mbsl. For all four holes at Site M0097 (Figures F10, F16), a mixed carbonate-volcaniclastic coarse-grained deposit, up to 1.81 m thick, occurs at the top of the succession. Below, coralgal-microbialite boundstone with dominantly branching and columnar *Porites* extends down to about 13.00 mbsf (Holes M0097A and M0097D) to 19.00 mbsf (Hole M0097C). Farther downhole, there are intervals of algal and microbialite-algal boundstone with thick coralline algal crusts and few corals, mainly branching *Porites*, down to about 20.00 mbsf (Holes M0097A and M0097D) and to about 30.00 mbsf (Hole M0097C). Below, coralgal-microbialite boundstone was recovered down to 58.42 mbsf; columnar *Porites* dominate in the upper part of this interval and branching *Porites* the lower.

The MSCL and other physical properties data indicate some variability likely related to variations in lithology, but there are no notable features and no apparent downhole trends.

A total of seven U-Th dates were measured on samples from Site M0097; three of these samples are rejected based on anomalous δ^{234}U initial values or anomalously high ^{238}U concentration. Of the remaining four samples, the dates span ~133–150 ky BP with no stratigraphic age inversions, although the date at the base of Hole M0097B indicates some stratigraphic inconsistency. However, broadly these dates are consistent with the interpretation of the MIS 6/7 age of this H2 terrace from prior studies (Webster et al., 2009).

7.1.1.3. Site M0099

Site M0099 consists of two subterraces, one at a water depth of ~132 m and another at ~147 mbsl (Figures F10, F16). Holes M0099A–M0099C are located on the shallower subterrace and are directly comparable. Based on the main lithologic changes, discontinuity surfaces, and/or changes in physical properties, three main lithostratigraphic intervals are identified. The first interval forms the uppermost 6 to 7 m of each hole. The basal boundary of the first interval is a hardened, blackened, and bioeroded surface in Hole M0099A that corresponds to a major lithologic change in the two other holes. This interval is coralgal-microbialite boundstone in Holes M0099A and M0099C but is dominated by microbialite-algal boundstone in Hole M0099B. The second interval, only present in Hole M0099C (7.05–21.60 mbsf) is dominated by microbialite-algal boundstone and is bounded at its base by a major facies change, also reflected in the physical properties data. The third interval, also present only in Hole M0099C (21.60–36.05 mbsf), is bounded at its base by a hardened and bored surface. This interval is divided into two main lithologies: an upper algal boundstone that overlies a coralgal boundstone with a coarse-grained biodetrital matrix.

Holes M0099E–M0099G are located on the lower (144–146 m water depth) subterrace. Four major lithostratigraphic intervals are identified. The first interval forms the uppermost 6 to 7 m of Holes M0099E and M0099F. The basal boundary of this interval is not marked by a distinct sedimentary structure, but a facies change occurs below. This interval is coralgal-microbialite boundstone in Hole M0099E but is composed of two lithologies in Hole M0099F: an upper algal boundstone that overlies a coralgal boundstone. The second interval, observed in Hole M0099E (5.86–15.15 mbsf) and Hole M0099F (7.08–12.97 mbsf) is dominated by microbialite-algal boundstone and algal boundstone and is bounded at its base by a major facies change, as well as a sharp change in physical properties. The third interval is present only in Hole M0099E (15.15–31.50 mbsf) and can be divided into two main lithologies: an upper coralgal boundstone that overlies an alternation of algal boundstone and unconsolidated, coarse-grained biodetrital sediment. The recovered material from Hole M0099G consists only of the fourth interval (30.89–48.40 mbsf) which is mainly composed of coralgal boundstone and algal boundstone. The contact with the basaltic substratum defines the basal boundary of this interval. The basaltic material in the lower parts of Hole M0099G represents coherent, in-place lava flows, hyaloclastite, and volcanic rubble, much of which is fresh and unaltered, although zones of substantial alteration occur in

both the coherent lava and the hyaloclastite. A significantly more phenocryst-rich lithology occurs in the lower sections of Hole M0099G.

The physical properties data, particularly the MSCL natural gamma radiation (NGR) and density data, suggest that there is a marked change at around 25 mbsf in Hole M0099C and at around 15 mbsf in Hole M0099E that may correlate with major changes in lithologies (i.e., microbialite-algal to boundstone in Hole M0099C and microbialite-algal to coralgal microbialite in Hole M0099E). The NGR values are relatively high and the density values are relatively low below these depths compared to those above.

A total of six samples for radiocarbon dates and seven samples for U-Th dates were measured on samples from Site M0099; two of the U-Th dates are rejected based on anomalously high ^{238}U concentrations. The radiocarbon dates and remaining five U-Th dates are in stratigraphic order and are consistent with the interpretation of the age of the H1 terrace spanning MISs 1–5 (Ludwig et al.,1991; Webster et al., 2009; Sanborn et al., 2017).

7.1.1.4. Site M0100
Site M0100 consists of one hole (M0100A) (Figures **F10**, **F16**) located at a water depth of 998 m and was drilled to 12.43 mbsf. This hole comprises an upper portion of coralgal boundstone underlain by a volcanic sequence of in-place lavas, welded volcanic breccias, and volcaniclastic sediments.

The MSCL resistivity, density, and magnetic susceptibility data from Hole M0100A vary considerably and may correspond to changes in the physical properties and/or chemistry of the basalts.

One U-Th date was obtained from a sample from Hole M0100A, yielding a date of ~329 ky BP, which is consistent with the estimated MIS 9 age for the H6 terrace (Ludwig et al., 1991; Webster et al., 2009 and references therein).

7.1.1.5. Site M0107
Site M0107 consists of one hole (M0107A) (Figures **F10**, **F16**) located at a water depth of 404 m and was drilled to 13.05 mbsf. This site represents a shallower subterrace of the H2 terrace that was also drilled at Site M0097.

Hole M0107A mostly recovered porphyritic basalt with high contents of olivine and clinopyroxene in an unaltered microcrystalline matrix disrupted by intervals of carbonate crust or carbonate sediment infilling. The basalt is directly overlain by a thin coralgal boundstone (10 cm thick) that in turn is capped by a conglomerate of mixed carbonate-volcaniclastic clasts.

The MSCL resistivity, density, and magnetic susceptibility data from Hole M0107A have notable variability that may correspond to changes in the physical properties and/or chemistry of the basalts.

One U-Th date was measured on a sample from Hole M0107A, yielding a date of ~130 ky BP. This date is consistent with the estimated MIS 6/7 age of the H2 terrace (Ludwig et al., 1991; Webster et al., 2007).

7.1.1.6. Site M0110
Site M0110 consists of two holes. Hole M0110A is located on the deeper subterrace at a water depth of 157 ms and Hole M0110B is located on the shallower subterrace at a water depth of 145 m (Figures **F10**, **F16**). The cored succession is divided into five lithologic intervals from top to bottom in Hole M0110A: (1) loose rhodoliths, (2) coralgal-microbialite boundstone, (3) biodetrital rudstone, (4) coralgal-microbialite boundstone, and (5) basalt. Intervals 1 and 2 are separated from Intervals 3–5 by a major lithologic boundary at 4.37 mbsf in Hole M0110A, and Intervals 3 and 4 are absent in Hole M0110B.

The MSCL NGR, density, and magnetic susceptibility data, as well as the L* data, from Holes M0110A and M0110B have notable downhole trends that reflect the transition from reef material above to basalt below. Relative to the reef facies, the basalt has lower L* and higher NGR, density,

and magnetic susceptibility, with notable variability that may correspond to changes in the physical properties and/or chemistry of the basalts.

Four radiocarbon dates were obtained from Site M0110. The uncalibrated radiocarbon dates span ~35–12 ky ^{14}C BP and are consistent with the estimated age of the H1 terrace that spans MISs 1–5 (Sanborn et al., 2017; Webster et al., 2009; Ludwig et al., 1991).

7.1.2. Mahukona sites

Sites M0098 and M0108 are located off shore the submerged Mahukona Volcano and intersect perhaps the most prominent reef structure (H8) on the northwest flank of Hawai'i (Figure **F11**). This feature is divided into two subterraces; dive observations, samples, and dredges show that these robust features are both coral reefs (H8a and H8b) (Webster et al., 2009), and previous U-series dating of three corals yielded ages of 360, 406, and 475 ka (Ludwig et al., 1991). Site M0098 penetrates the upper reef (H8a) at a water depth of 1100 m, and Site M0108 penetrates the lower reef (H8b) at a water depth of 1177 m. At a water depth of 1242 m, M0109 penetrates the deepest (H9) of the reefs sampled during Expedition 389.

7.1.2.1. Site M0098

At Site M0098, one hole was drilled at a water depth of 1100 m to 19.22 mbsf (Figures **F11**, **F17**). Based on the main lithologic changes and discontinuity surfaces, four main intervals are identified. Interval 1 consists of coralgal boundstone from 0 to 0.35 mbsf and is bounded at its base by a major facies change. Interval 2 consists of unconsolidated sediments, coralgal boundstone, and consolidated grainstone from 0.35 to 1.97 mbsf. This interval is bounded at its base by a major facies change. Interval 3 consists of coralgal boundstone from 1.97 to 11.04 mbsf and is bounded at its base by another facies change. Interval 4 consists of coralgal-microbial boundstone from 11.04 to 19.22 mbsf.

Because of poor recovery and drilling disturbance, there is only sparse physical properties data and there are no apparent downhole trends.
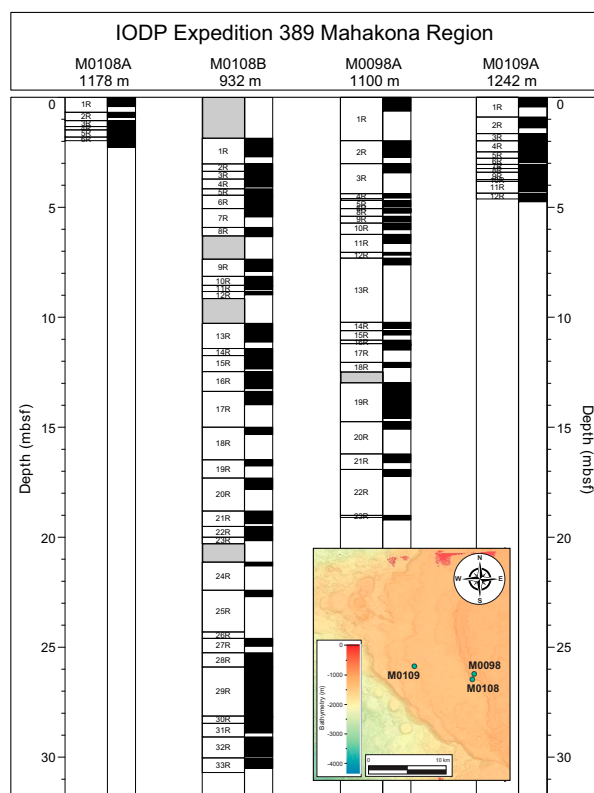

Figure F17. Mahukona region cores and recovery for Sites M0098, M0108, and M0109, with site location maps overlain on a 10 m grid bathymetric map (**https://www.ncei.noaa.gov/maps/bathymetry**).

Two U-Th dates were measured on samples from Hole M0098A spanning ~410–421 ky BP, which is consistent with the estimated age of the H8 terrace (Ludwig et al., 1991; Webster et al., 2009).

7.1.2.2. Site M0108

Site M0108 consists of two holes (M0108A and M0108B) located on the same subterrace at a water depth of 1178 m (Figures **F11**, **F17**). Based on the main lithologic changes, three main lithostratigraphic intervals are identified from top to bottom. The upper interval, spanning all of Hole M0108A and 1.86 to 8.83 mbsf of Hole M0108B, is dominated by coralgal-microbialite boundstone and characterized by robust branching *Porites*. The second interval, recovered only in Hole M0108B from 8.83 to 25.25 mbsf, is composed predominantly of highly fragmented coralgal boundstone embedded locally in a biodetrital matrix. The lower interval, from 25.25 mbsf to the base of Hole M108B at 30.70 mbsf, consists mostly of an unconsolidated coarse-grained biodetrital sediment with abundant loose reworked large *Porites* and *Montipora* clasts, as well as crustose coralline algal fragments.

Because of poor recovery and drilling disturbance, there are only sparse physical properties data and no apparent downhole trends.

Four samples were U-Th dated, but the topmost sample from Hole M0108A is rejected based on an anomalously high $\delta^{234}U$ concentration (>4 ppm) and an anomalously high $\delta^{234}U$ initial value (>160‰). The remaining three samples are from Hole M0108B and provide dates spanning ~364–472 ky BP, although the lower two samples reveal an age inversion. Overall, these dates are consistent with the timing of stratigraphically adjacent terrace development shown in Webster et al. (2009) and with the ages and depths of dated corals in Ludwig et al. (1991).

7.1.2.3. Site M0109

Site M0109 consists of one hole (M0109A) located at a water depth of 1241.8 m (Figures **F11**, **F17**). Below a thin interval of unconsolidated biodetrital sediment, Hole M0109A consists of highly disturbed coralgal boundstone comprising mostly branching and columnar *Porites* with thin coralline algal crusts.

Because of poor recovery and drilling disturbance, there are only sparse physical properties data and no apparent downhole trends.

Two U-Th dates were obtained from Hole M0109A, but both are rejected based on anomalous $\delta^{234}U$ initial values (below 130‰ or above 160‰), and one of the dates also has high uncertainty due to being near secular equilibrium. Site M0109 is the deepest site drilled during Expedition 389, and thus presumably has the oldest reef material, which is close to the limit of U-Th dating.

7.2. Windward side

7.2.1. Kohala sites

Two sites (M0101 and M0102) were drilled offshore Kohala on the northeast side of Hawai'i. Site M0101 intersects the prominent reef terrace (H7) at 930 mbsl that is well exposed by a submarine plunge pool system (Webster et al., 2009) (Figure **F12**). Site M0102, selected on the basis of the bathymetric/backscatter data, intersects the reef (H2d) at 410 mbsl, also targeted on the leeward side Kawaihae region (Site M0097) and at another windward location in the Hilo region (Sites M0103 and M0104).

7.2.1.1. Site M0101

Two holes were drilled at Site M0101 (Holes M0101A and M0101B) at water depths of ~932 m to a total depth of 45 mbsf (Figures **F12**, **F18**). In both holes, core material consists, from top to bottom, of a 30–50 cm thick interval of brecciated basalt, an interval of consolidated and unconsolidated bioclastic material extending to ~5 mbsf, and a coralgal microbialite boundstone composed predominantly of laminar and branching *Porites* with thin crustose coralline algal crusts overlain by thin microbialite crusts. In Hole M0101B, beneath the coralgal microbialite boundstone at ~25 mbsf, there is a ~3.5 m thick layer of unconsolidated biodetrital sediment. Below that layer, basalt extends to the bottom of the hole at ~ 45 mbsf.

The MSCL NGR, density, and magnetic susceptibility data, as well as the L* data, from Site M0101 show notable downhole trends that reflect the transition from reef material above to basalt below. Relative to the reef lithologies, the basalt has lower L* and NGR and higher density and magnetic susceptibility, and it has notable variability that may correspond to changes in the physical properties and/or chemistry of the basalts.

A total of five U-Th dates were obtained for Site M0101. One date is rejected on the basis of anomalously high $\delta^{234}U$ concentration. Replicates were run on one sample, which yielded the same date within the reported uncertainty. There is one age inversion between two samples. Overall, the dates span ~365–434 ky BP, consistent with the estimated age of the H7 terrace (Ludwig et al., 1991; Webster et al., 2009).

7.2.1.2. Site M0102

Two holes were drilled to ~73 mbsf at Site M0102 (Holes M0102A and M0102C) at water depths of 413–416 m (Figures **F12**, **F18**). Based on the main lithologic changes and discontinuity surfaces, four main lithostratigraphic intervals are identified. Interval 1 forms the major part of Hole M0102A (0–22.25 mbsf) and consists of rhodolith floatstone embedded in unconsolidated biodetrital-volcaniclastic sediment. The basal boundary corresponds to a lithology change in both Holes M0102A and M0102C. Interval 2, recovered from 22.25 to 24.61 mbsf in Hole M0102A and from 21.58 to 28.85 mbsf in Hole M0102C, is dominated by coralgal boundstone with submassive to massive *Porites*. At its base, it is bounded by a thin layer of consolidated, biodetrital, coarse-grained rudstone to grainstone. Interval 3 is a succession of coralgal microbialite boundstone from 29.25 to 70.69 mbsf in Hole M0102C (not recovered in Hole M0102A), with coral morphologies and types changing downward from branching and platy *Porites* and columnar *Pavona* to predominantly very large massive *Porites* with rare laminar *Pavona*. Interval 4, from 70.69 to 72.71 mbsf in Hole M0102C (not recovered in Hole M0102A), consists of coralgal boundstone with numerous branching and platy *Porites*.
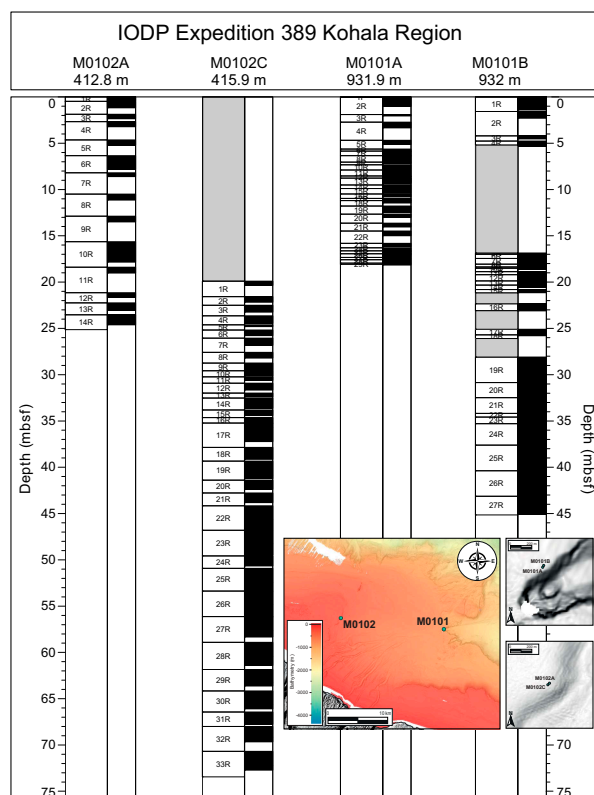

Figure F18. Kohala region cores and recovery for Sites M0101 and M0102, with site location maps overlain on a 10 m grid bathymetric map (**https://www.ncei.noaa.gov/maps/bathymetry**).

The MSCL NGR, density, and magnetic susceptibility data, as well as the L* data, at Site M0102 do not have any apparent downhole trends, although there is a notable downhole increase in the range of values in all these parameters below about 40 mbsf.

Five U-Th dates were measured on samples from Site M0102 that span ~171–225 ky BP. None of these dates was rejected on the basis of the U-Th geochemistry; however, there is one age inversion near the bottom of Hole M0102C. Overall, the dates from Site M0102 are consistent with the timing of development of the H2 terrace spanning MIS 6/7 from Webster et al. (2009).

7.2.2. Hilo sites

Three sites (M0103–M0105) were drilled off shore Hilo on the east side of Hawai'i (Figure **F13**). Submersible dive observations and samples confirm that the targeted features are coral reefs that likely span MISs 1–5 and 6–7 (Puga-Bernabéu et al., 2016). Site M0103 targeted the ~400 mbsl reef (H2d), which was also cored at Kawaihae (Site M0097) and Kohala (Site M0102). Site M0104 was drilled at a shallower water depth of 347 m where high backscatter was mapped and carbonate mounds (pinnacles) were described (Puga-Bernabéu et al., 2016). Finally, Site M0105 was drilled upslope from Site M0104 on a subterrace at a water depth of 340 m.

7.2.2.1. Site M0103

Site M0103 consists of one hole (M0103A) located at a water depth of 405 m (Figures **F13**, **F19**). Core material consists predominantly of pebble- to cobble-sized rhodoliths in the uppermost 26.60 m of the hole. The lower part, below 26.60 mbsf, is mostly composed of unconsolidated biodetrital sediment with foliaceous corals, including *Leptoseris*, down to 37.60 mbsf and up to cobble-sized fragments of massive *Porites* below. At 42.20 mbsf, a contact with basalt breccia was recovered down to the bottom of the hole at 44.78 mbsf.

The poor recovery for Hole M0103 makes it difficult to detect downhole trends in the physical properties data. However, there is a notable peak in the magnetic susceptibility data at the litho-
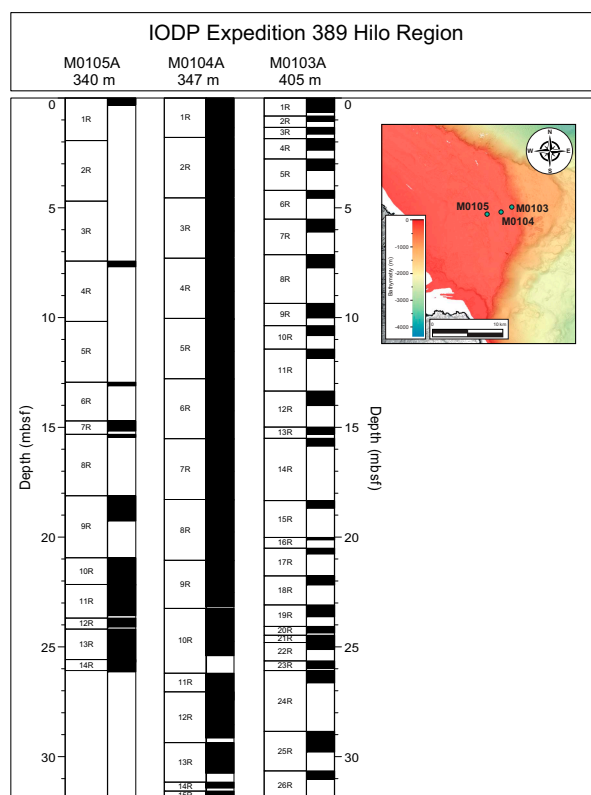

Figure F19. Hilo region site cores and recovery (Sites M0103–M0105), with site location maps overlain on a 10 m grid bathymetric map (**https://www.ncei.noaa.gov/maps/bathymetry**).

logic boundary at 26.60 mbsf, and there is variability in the L* data that may correspond to changes in lithology (e.g., rhodolith rudstone/floatstone to algal boundstone).

Four U-Th dates were obtained from Hole M0103A that span ~138–216 ky BP. The dates are in stratigraphic order and are consistent with the interpretation of the age of the H2 terrace spanning MISs 6 and 7 (Ludwig et al., 1991; Webster et al., 2009).

7.2.2.2. Site M0104
Site M0104 consists of one hole located at a water depth of 347 m (Figures **F13**, **F19**). Hole M0104A spans 0–46.15 mbsf, and based on the main lithologic changes, discontinuity surfaces, and/or changes in physical properties, it is possible to identify five main lithostratigraphic intervals. Interval 1 is formed by the upper consolidated biodetrital grainstone to rudstone, from 0 to 0.80 mbsf, and is bounded at its base by a major facies change and by a change in physical properties. Interval 2 forms the largest part of the hole and consists predominantly of coralgal microbial boundstone from 0.80 mbsf to 31.81 mbsf with occurrences of thin sections of microbial-algal boundstone and algal boundstone. The base of this interval is a blackened, hardened, and bored surface with a sharp change in physical properties. Interval 3 is composed of consolidated biodetrital grainstone and algal boundstone (with occasional coralgal grainstone) from 31.81 to 39.87 mbsf, and it is bounded at its base by a major facies change, as well as a change in physical properties. The base of this interval is a heavily bored surface. Interval 4 comprises coralgal boundstone, algal boundstone, and biodetrital grainstone facies from 39.87 to 43.39 mbsf. The top is capped by rhodoliths, and the base is marked by a coralgal boundstone. The base is defined by major changes in both facies and physical properties. Interval 5 consists of biodetrital grainstone and algal boundstone from 43.39 to 46.15 mbsf.

The boundaries between lithologic intervals have marked changes in physical properties: a decrease in magnetic susceptibility and an increase in L* values at the base of Interval 1, a trend from dominantly high L* values to more variable L* values within Interval 2 and a striking increase in magnetic susceptibility values from about 20 mbsf to the highest values at the base of Interval 2, relatively low magnetic susceptibility values in Interval 3, relatively low magnetic susceptibility and relatively high and less variable L* values in Interval 4, and a slight increase in magnetic susceptibility values in Interval 5.

A total of three U-Th dates were obtained from corals from Hole M0104A and span ~130–159 ky BP with no stratigraphic age reversals. These dates are consistent with the estimated age of the H2 terrace spanning MIS 6/7 (Ludwig et al., 1991; Webster et al., 2009).

7.2.2.3. Site M0105
Site M0105 consists of one hole located at a water depth of 340 m (Figures **F13**, **F19**). Based on the main lithologic changes, Hole M0105A can be divided into four main lithostratigraphic intervals. The top interval is rhodoliths in a dark gray unconsolidated biodetrital and volcaniclastic sandy matrix, and the second interval is dominated by algal boundstone around 7.5 mbsf. Because of poor recovery, the vertical extent and the boundaries of this interval are unknown. The third interval, only recovered from 7.69 to 12.95 mbsf, is dominated by a fragmented coralgal boundstone (predominantly columnar and robust branching *Porites*) embedded in unconsolidated biodetrital background sediments. The fourth interval represents lava flows and basalt clinker, which is usually produced on the top and leading edge of 'a'a lava flows, much of which is fresh and unaltered, although zones of fracturing and alteration occur locally.

In the upper three lithologic intervals of reef material, poor recovery makes it difficult to detect downhole trends in the physical properties data. However, there are notable changes in the MSCL and L* data that reflect the transition from reef material above to basalt below. Relative to the reef lithologies, the basalt has lower L* and higher density and magnetic susceptibility, notable variability that may correspond to changes in the physical properties and/or chemistry of the basalts.

There are two U-Th dates for Hole M0105A, both ~132 ky BP, consistent with the previously-inferred timing of formation of the H2 terrace spanning MIS 6/7 (Webster et al., 2009; Puga-Bernabéu et al., 2016).

7.2.3. Ka Lae site

Because of the denial of permit applications to sample the H1d reef in Hawaiian state waters at any of the planned locations on the leeward (Kawaihae and Kona) and windward (Hilo) sides, a request was made and permission received from the IODP Site Survey Panel and EPSP to add a site on the H1d reef in the Ka Lae region (South Point). This was the only location available to drill on the H1d reef on the windward side of Hawai'i that was located in federal waters (Figure **F14**). The site survey data at Ka Lae is limited. To select the drilling location of Site M0106, we used the available bathymetric data and the information from two HURL submersible dives (P5-77 and P5-78), including images, pilot logs, and descriptions and locations of collected carbonate rocks (see Webster et al., 2004 for references).

7.2.3.1. Site M0106

Two holes were drilled to ~16 mbsf at Site M0106 (Holes M0102A and M0102B) at water depths of ~148 m (Figures **F14**, **F20**). Core material recovered from Site M0106 consists mostly of loose rhodoliths with crustose and fruticose coralline algal crusts down to 11.50 mbsf. Below this depth in Hole M0106B, a 1.30 m section of unconsolidated biodetrital sediment contains pebble-sized rhodoliths and coral clasts in a finer bioclastic matrix that overlies a coralgal boundstone with massive *Porites*.

The poor recovery at Site M0106 makes it difficult to detect downhole trends in the physical properties data. However, there is a notable increase in the L* data that may correspond to changes in lithology at 11.50 mbsf from rhodoliths to coralgal boundstone.

Two radiocarbon dates were obtained from Site M0106, and they span 27–35 ^{14}C ky BP. The dates are consistent with the interpretation of the age of the H1 terrace spanning MISs 1–5 (Webster et al., 2009; Ludwig et al., 1991).
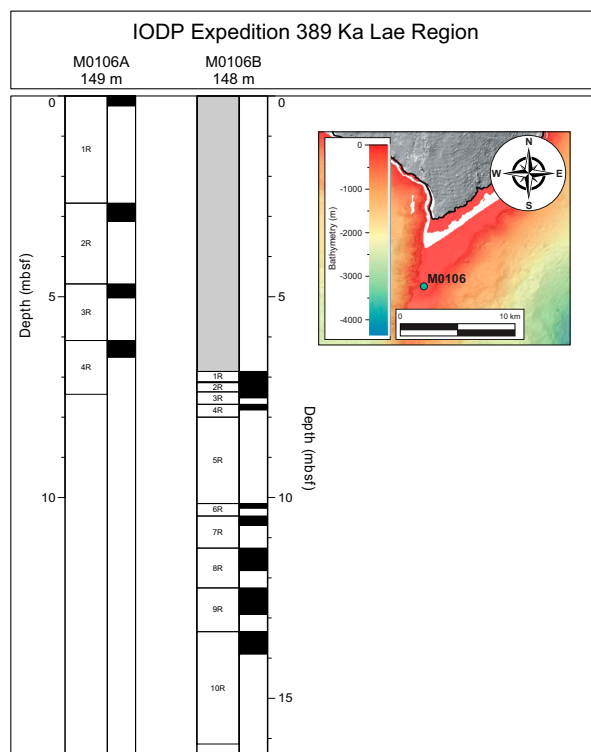

Figure F20. Ka Lae region cores and recovery for Site M0106, with site location map overlain on a 10 m grid bathymetric map (**https://www.ncei.noaa.gov/maps/bathymetry**).

8. Geochemistry

Sixteen surface seawater samples were collected during the offshore phase of Expedition 389, one at each of the 15 drill sites and an additional sample at the location of Site M0099, using an improvised sampling device or a 2L Niskin bottle. Parameters including salinity, pH, alkalinity, and ammonium concentrations were analyzed offshore, and major cations and anions were measured during the OSP. Results for all parameters fall within the expected ranges for surface seawater.

A total of 36 interstitial water samples were collected from all intervals with sufficient undisturbed soft sediment using Rhizon samplers during the offshore phase of Expedition 389. Two samples are from Site M0099, 14 are from Site M0101, 14 are from Site M0102, 3 are from Site M0103, and 2 are from Site M0105. Parameters including salinity, pH, alkalinity, and ammonium concentrations were analyzed offshore, and major cations and anions were measured during the OSP. Downhole trends are only apparent at Sites M0101 and M0102, where most of the measurements were made. At Site M0101, there are notable downhole trends in sulfate, strontium, manganese, chloride, and barium. At Site M0102, there are downhole trends in pH and ammonium, calcium, strontium, and silicate. Future work may identify the processes responsible for these downhole trends.

Rock and sediment samples from all sites were taken during the OSP for IODP standard measurements. In total, 144 samples were analyzed for bulk composition using energy dispersive X-Ray fluorescence (ED-XRF). In addition, splits of those samples were analyzed for total carbon (TC) and total organic carbon (TOC) using a carbon-sulfur analyzer, and total inorganic carbon (TIC) was calculated as the difference between TC and TOC. The set of 144 samples comprises 3 from Site M0096, 31 from Site M0097, 3 from Site M0098, 22 from Site M0099, 1 from Site M0100, 10 from Site M0101, 14 from Site M0102, 6 from Site M0103, 9 from Site M0104, 2 from Site M0105, 2 from Site M0106, 2 from Site M0107, 4 from Site M0108 and 5 from Site M0110. Because of the short length of the core, no bulk samples for geochemistry were taken from Site M0109.

The bulk composition results primarily reflect large differences between samples from fossil reef compared to samples from basalt intervals. As such, the sites at which basalt was recovered (M0096, M0099, M0100, M0101, M0105, M0107, and M0110) have a large range of bulk compositions exemplified by the contrast between relatively high concentrations of calcium in the fossil reef facies samples compared to the relatively low concentrations of calcium and high concentrations of aluminum, iron, manganese, and silica in the basalt samples. The bulk geochemical data can be used to divide the reef facies samples into two groups characterized by their location on the leeward versus windward sides of Hawai'i. Aluminum, iron, manganese, and silica concentrations are below detection limit in reef facies samples from all the leeward/dry sites and some of the windward sites, but these elements have modest to moderate concentrations, relative to pure basalt samples, in reef facies samples from several of the windward/wet sites (M0101, M0102, and M0104).

As expected, the TC and TOC weight percent values primarily reflect large differences between samples from reef facies compared to samples from basalt intervals. There is some variability within the data from reef facies samples, with typical values ranging 11–12 wt% TC, and 0.1–0.2 wt% TOC.

9. Paleomagnetism

Approximately one plug sample per core section, and in a few cases sediment cubes, were obtained from all sites except for Sites M0108 and M0109 during the OSP, for a total of 308 samples (301 plugs and 7 cubes). The lack of cohesive material due to drilling disturbance prevented paleomagnetic sampling for Sites M0108 and M0109. Measurements of low-field and mass-specific magnetic susceptibility (χ) were carried out for all samples. Natural remanent magnetization (NRM) was measured for all plug samples, as well as remanence following stepwise alternating field (AF) demagnetization up to a peak AF of 20 mT and for basalt samples up to 100 mT. The samples are

from two main lithologies: reef carbonates and basalts. A total of 193 samples are carbonate, and the remaining 105 are basalt.

Across all the Expedition 389 sites, χ values range -2.73×10^{-8} to 1.31×10^{-4} m³/kg and initial NRM intensity values range 4.50×10^{-7} to 5.89×10^{-1} A/m. This range generally reflects the differences in lithology, with basalts having higher χ values and higher NRM intensity values compared to carbonates. These differences are clearly seen in data from Sites M0096, M0097, M0099, M0101, M0102, M0105, and M110, where both carbonate and basalt samples were analyzed. To get an idea of end-member values, sites where only basalt samples were analyzed can be compared to sites where only carbonate samples were measured; sites with only basalt samples (Sites M0100 and M0107) have an arithmetic mean χ value of 7.07×10^{-6} m³/kg and an arithmetic mean initial NRM value of 6.07×10^{-2} A/m, compared to sites with only carbonate samples (Sites M0098, M0103, M0104, and M0106), which have an arithmetic mean χ value of 1.86×10^{-7} m³/kg and an arithmetic mean initial NRM value of 1.93×10^{-4} A/m.

Visual inspection of the data indicates that χ values covary with initial NRM values at most sites in both carbonate and basaltic intervals, suggesting that magnetic mineral concentrations may drive downhole variations in both parameters. However, there are exceptions in some carbonate intervals where no covariance is apparent, probably as an artifact of very low mineral concentrations. In addition, data from Hole M0110B show that χ does not co-vary with initial NRM, possibly reflecting changes in magnetic grain size.

There are site-to-site differences in χ values measured within carbonate samples that may reflect differences in the contribution and incorporation of volcanic sediment into the reef facies. This is apparent when comparing measurements of carbonate samples from the windward/wet Sites M0101, M0102, and M0103 to the leeward/dry Sites M0097, M0098, M0099, and M0110: the carbonate samples from the windward/wet site have maximum χ values up to 9.92×10^{-6} m³/kg, approximately three orders of magnitude higher than the maximum χ values from carbonate samples from the leeward/dry sites.

10. Preliminary scientific assessment

10.1. Objective 1: to define the nature of sea level change in the central Pacific over the last 500 ky

We aim to reconstruct the most complete and detailed sea level record from fossil corals, particularly into, during, and out of the glacial periods. These data will allow more detailed testing of the sensitivity and vulnerability of ice sheet responses to orbital to millennial-scale climate change. A sea level curve will be built using absolute radiometric dating methods (^{14}C accelerator mass spectrometry [AMS] <50 ka and U/Th) of in situ corals, paleobathymetric data, and published and directly calculated subsidence rates for Hawai'i.

The offshore phase successfully recovered cores from the succession of fossil reef terraces (H1, H2, H4, H6, H7, H8, and H12) between 130 and 1240 mbsl. Initial observations of the 340 m of fossil reef cores and reconnaissance radiometric dating reveal that the archives span the past 500,000 y. The preliminary data also suggest we recovered sequences indicative of reef growth and demise during numerous periods of major ice sheet and sea level instability (e.g., MIS 12-11, MIS 10-9, MIS 7-5, MIS 3, and MIS 2-1). During the OSP, high-quality fossil coralgal samples, consistent with shallow, high-energy settings, were taken for dating and sea level change investigations, the results of which are expected to contribute to Objective 1.

10.2. Objective 2: to reconstruct paleoclimate variability for the last 500 ky and establish the relationship between the mean climate state and seasonal–interannual variability

We aim to use coral-derived temperature and precipitation records to investigate how high-latitude climate (e.g., ice sheet size), atmospheric CO_2 levels, and mean and seasonal solar radiation

impact Hawaiian climate including storminess and the position of the Intertropical Convergence Zone. In combination with theoretical studies of subtropical climate change, these records will allow for the identification and study of critical processes that determine Pacific-wide climate.

The offshore phase successfully recovered massive, submassive, and columnar *Porites* spp. coral colonies that are potentially suitable for paleoclimate studies. Most of the specimens that can be used for monthly-resolution, multidecadal paleoclimate reconstructions are from the H1 and H2 terraces; preliminary dates indicate these samples are probably from MISs 3, 6, and 7. There is also a high abundance of smaller specimens that represent <15 y of growth found throughout the recovered reef sections. At the OSP, >200 samples were taken for paleoclimate analyses. Overall, preliminary assessment of the quality and possible ages of the suite of corals specimens recovered during Expedition 389 suggest they grew during past periods with a wide dynamic range of climate forcing boundary conditions and thus will contribute to Objective 2.

10.3. Objective 3: to establish the geologic and biological response of coral reef systems to abrupt sea level and climate changes

We aim to reconstruct the detailed stratigraphic, geomorphic, and paleoenvironmental evolution of each reef in response to abrupt sea level and climate changes; test ecological theories about coral reef resilience and vulnerability to past and future climate changes by assessing the nature and rate of change in reef communities within and between successive reefs over interglacial–millennial timescales; and establish the nature of living and ancient microbial communities in the reefs and their role in reef building.

The offshore phase successfully recovered fossil reef cores from reef terraces at a range of water depths and ages from five different geographic areas around the island, representing both the leeward/dry and windward/wet sides of Hawai'i. Therefore, analyses of samples taken during the OSP will be interpreted in a broad spatial-temporal context, which will allow a rich understanding of the development of the Hawaiian reef system in response to major environmental changes over the past 500 ky. Preliminary observations of the cores confirm a diverse suite of lithologies and facies (mixtures of coralgal material, microbialite, and sediments) representing various shallow to deep depositional reefs settings, as well the numerous, major lithologic boundaries indicating repeated reef initiation and demise that when investigated further will contribute to Objective 3.

10.4. Objective 4: to elucidate the subsidence and volcanic history of Hawai'i

We aim to refine the variation through space and time of the subsidence of Hawai'i and contribute to understanding the volcanic evolution of the island. The key to this objective is to obtain well-dated volcanic samples from the base of each hole and interbedded within or draping over the reefs.

During the offshore phase, volcanic eruption products were recovered from numerous sites and from nearly all geographic areas studied (all but Ka Lae). These volcanic products, primarily lava flows, were found on top of, within (interbedded), and beneath the reef terraces sampled during the expedition. These materials are sufficient to deduce eruption conditions (subaerial, littoral, and submarine) and deposit distance from volcanic vents. Given the preliminary ages of associated reef material, these lava flows likely date to a time period that is not well represented on the island of Hawai'i and will therefore be critical for reconstructing the Late Pleistocene geological history of Hawai'i.

11. Outreach

The overall aim of the ESO Outreach and Education effort is to promote the science of each expedition and the wider objectives of IODP and ECORD to a broad audience, including the scientific community and general public. To accomplish this objective, the outreach goals were to publicize

the aims of the expedition and initial results to media outlets, IODP offices, communication departments of science party members, and social media.

11.1. Targeted activities

The expedition web page on the ECORD website was used as a source of information by including daily and weekly offshore reports and links to the blog. The website also includes links to expedition materials and a media pack with information about media releases along with pictures and contact details to arrange interviews with the expedition scientists.

In total, 28 articles were posted on Expedition 389's blog (3 pre-offshore, 18 offshore, and 7 onshore). The blog was visited nearly 13,000 times between June 2023 and March 2024. Visitors came mostly from Germany, the U.S.A., Australia, the United Kingdom, India, Japan, France, Netherlands, Italy, and Spain.

All Science Party members were encouraged to contact and inform the communications departments of their home institutions before the offshore and the onshore phases of the expedition. The aim was to raise awareness of their staff's participation in the expedition locally and nationally.

Expedition promotional materials, including an expedition logo and flier, as well as branded items such as caps, T-shirts, iron-on patches, and stickers, were available during the offshore phase. Banners with the IODP and ECORD logos and the expedition logo were displayed on board the *MMA Valour* during the offshore phase. Widespread use of logos was documented in photographs and videos.

Two embargoed press releases were issued, one before the offshore phase and one toward the end of the OSP. Both were shared with all science party members' communication departments including the Australia-New Zealand IODP Consortium (ANZIC), the U.S. Science Support Program (USSSP), and all ECORD entities. The press releases were also distributed via EurekAlert and idw (Informationsdienst Wissenschaft/Germany). Two media days were held, and invitations were issued to local and regional media both on Hawai'i just before embarking the vessel and in Bremen toward the end of the onshore phase. One interested person but no media participants attended prior to the offshore phase. The media day during the OSP was attended by the largest newspaper in the region as well as a local television station. A wider audience was reached with more personalized news items on Science Party members institution's homepages and personalized media releases as well as individual social media engagement by the science party.

An Onboard Outreach Officer (OOO) (Marley Parker) was chosen by the ECORD outreach task force (EOTF) in July 2023. During the first leg of the offshore phase, the OOO participated off shore and took pictures, wrote feature stories for the blog, and posted short insights about the expedition to ECORD social media channels. These activities continued during the second leg of the expedition and after the offshore phase. A short film was produced onboard the *MMA Valour* and shared on YouTube to give insights about living aboard a research vessel and the scientific objectives of the expedition. The OOO attended the first half of the OSP in Bremen and, assisted by EOTF members, wrote features for the expedition blog, documented the tasks of the science party in pictures, and undertook filming for a short film about the expedition featuring six science party members, highlighting the international nature of the program and including representation of all IODP expedition operators.

11.2. Community engagement

Prior to the expedition, there was insufficient community engagement with the native and local Hawaiian community, which was the primary reason for being denied permits to operate in Hawai'i state waters, thereby compromising some important expedition objectives. The lack of trust building with the Hawaiian community also caused internal feelings of dissonance in many scientists who are committed both to social justice and to the expedition's scientific objectives. During the active offshore operational phase, a 10 minute Q&A video was produced and published on the expedition website addressing questions about the expedition science and the active offshore phase of the expedition. Interview requests during the offshore phase were met by the Co-

Chief Scientists and included an interview for regional television news. During the offshore phase, local community members and interested parties were invited to join an online meeting on 5 October 2023; however, there were no attendees. Following the conclusion of the offshore phase, and in response to not gaining the permits required to operate in Hawaiian state waters, ESO published a statement on the expedition website (see below) regarding community engagement on Hawai'i.

11.3. Media and expedition links

- Expedition website: **https://ecord.org/expedition389**
- Expedition blog: **https://expedition389.wordpress.com**
- Offshore Q&A video: **https://youtu.be/-cuAgrmG8ho?si=YU0bB25jaQA96zv0**
- Butenunbinnen (regional television program on radio Bremen): **https://www.butenunbin-nen.de/videos/klima-forschung-hawai-bremen-100.html**

References

Berger, A., and Loutre, M.F., 1991. Insolation values for the climate of the last 10 million years. Quaternary Science Reviews, 10(4):297–317. **https://doi.org/10.1016/0277-3791(91)90033-Q**

Campbell, J.F., 1986. Subsidence rates for the Southeastern Hawaiian Islands determined from submerged terraces. Geo-Marine Letters, 6(3):139–146. **https://doi.org/10.1007/BF02238084**

Chappell, J., 2002. Sea level changes forced ice breakouts in the Last Glacial cycle: new results from coral terraces. Quaternary Science Reviews, 21(10):1229–1240. **https://doi.org/10.1016/S0277-3791(01)00141-X**

Clague, D.A., and Moore, J.G., 1991. Geology and petrology of Mahukona Volcano, Hawaii. Bulletin of Volcanology, 53(3):159–172. **https://doi.org/10.1007/BF00301227**

Clague, D.A., Reynolds, J. R., Maher, N., Hatcher, G., Danforth, W., and Gardner, J. V., 1998. High-resolution Simrad EM300 Multibeam surveys near the Hawaiian Islands: canyons, reefs, and landslides. Eos, Transactions of the American Geophysical Union, 79:F826.

Dai, A., Fyfe, J.C., Xie, S.-P., and Dai, X., 2015. Decadal modulation of global surface temperature by internal climate variability. Nature Climate Change, 5(6):555–559. **https://doi.org/10.1038/nclimate2605**

Dartnell, P., and Gardiner, J.V., 1999. Sea-floor images and data from multibeam surveys in San Francisco Bay, Southern California, Hawaii, the Gulf of Mexico, and Lake Tahoe, California-Nevada. U.S. Geological Survey. Data Series. **https://doi.org/10.3133/ds55**

Galewsky, J., Silver, E.A., Gallup, C.D., Edwards, R.L., and Potts, D.C., 1996. Foredeep tectonics and carbonate platform dynamics in the Huon Gulf, Papua New Guinea. Geology, 24(9):819–822. **https://doi.org/10.1130/0091-7613(1996)024<0819:FTACPD>2.3.CO;2**

Hibbert, F.D., Rohling, E.J., Dutton, A., Williams, F.H., Chutcharavan, P.M., Zhao, C., and Tamisiea, M.E., 2016. Coral indicators of past sea-level change: a global repository of U-series dated benchmarks. Quaternary Science Reviews, 145:1–56. **https://doi.org/10.1016/j.quascirev.2016.04.019**

Humblet, M., and Webster, J.M., 2017. Coral community changes in the Great Barrier Reef in response to major environmental changes over glacial-interglacial timescales. Palaeogeography, Palaeoclimatology, Palaeoecology, 472:216–235. **https://doi.org/10.1016/j.palaeo.2017.02.003**

Imbrie, J., Hays, J.D., Martinson, D.G., McIntyre, A., Mix, A.C., Morley, J.J., Pisias, N.G., Prell, W.L., and Shackleton, N.J., 1984. The orbital theory of Pleistocene climate : support from a revised chronology of the marine $\delta^{18}O$ record. Proceedings of the NATO Advanced Research Workshop, 1984:269. **https://ui.adsabs.harvard.edu/abs/1984mcur.conf..269I**

Kavanaugh, M.T., Church, M.J., Davis, C.O., Karl, D.M., Letelier, R.M., and Doney, S.C., 2018. ALOHA from the edge: reconciling three decades of in situ Eulerian observations and geographic variability in the North Pacific subtropical gyre. Frontiers in Marine Science, 5. **https://doi.org/10.3389/fmars.2018.00130**

Köhler, P., Knorr, G., Stap, L.B., Ganopolski, A., de Boer, B., van de Wal, R.S.W., Barker, S., and Rüpke, L.H., 2018. The effect of obliquity-driven changes on paleoclimate sensitivity during the Late Pleistocene. Geophysical Research Letters, 45(13):6661–6671. **https://doi.org/10.1029/2018GL077717**

Lambeck, K., and Chappell, J., 2001. Sea level change through the last glacial cycle. Science, 292(5517):679–686. **https://doi.org/10.1126/science.1059549**

Lambeck, K., Esat, T.M., and Potter, E.-K., 2002. Links between climate and sea levels for the past three million years. Nature, 419(6903):199–206. **https://doi.org/10.1038/nature01089**

Lea, D.W., Martin, P.A., Pak, D.K., and Spero, H.J., 2002. Reconstructing a 350 ky history of sea level using planktonic Mg/Ca and oxygen isotope records from a Cocos Ridge core. Quaternary Science Reviews, 21(1):283–293. **https://doi.org/10.1016/S0277-3791(01)00081-6**

Ludwig, K.R., Szabo, B.J., Moore, J.G., and Simmons, K.R., 1991. Crustal subsidence rate off Hawaii determined from $^{234}U/^{238}U$ ages of drowned coral reefs. Geology, 19(2):171–174. **https://doi.org/10.1130/0091-7613(1991)019<0171:CSROHD>2.3.CO;2**

MBARI Mapping Team, 2000. MBARI Hawaii Multibeam Survey, Digital Series No. 2. Monterey Bay Aquarium Research Institute. **https://www3.mbari.org/data/mapping/hawaii/index.htm**

Moore, J.G., and Clague, D.A., 1992. Volcano growth and evolution of the island of Hawaii. Geological Society of America Bulletin, 104(11):1471–1484. **https://doi.org/10.1130/0016-7606(1992)104%3C1471:VGAEOT%3E2.3.CO;2**

Moore, J.G., and Fornari, D.J., 1984. Drowned reefs as indicators of the rate of subsidence of the Island of Hawaii. The Journal of Geology, 92(6):752–759. **https://doi.org/10.1086/628910**

Puga-Bernabéu, Á., Webster, J.M., Braga, J.C., Clague, D.A., Dutton, A., Eggins, S., Fallon, S., Jacobsen, G., Paduan, J.B., and Potts, D.C., 2016. Morphology and evolution of drowned carbonate terraces during the last two interglacial cycles, off Hilo, NE Hawaii. Marine Geology, 371:57–81. **https://doi.org/10.1016/j.margeo.2015.10.016**

Sanborn, K.L., Webster, J.M, Yokoyama, Y., Dutton, A., Braga, J.C., Clague, D.A., Paduan, J.B., Wagner, D., Rooney, J.J., and Hansen, J.R., 2017. New evidence of Hawaiian coral reef drowning in response to meltwater pulse-1A. Quaternary Science Reviews, 175:60–72. **https://doi.org/10.1016/j.quascirev.2017.08.022**

Schellmann, G., and Radtke, U., 2004. A revised morpho- and chronostratigraphy of the Late and Middle Pleistocene coral reef terraces on Southern Barbados (West Indies). Earth-Science Reviews, 64(3):157–187. **https://doi.org/10.1016/S0012-8252(03)00043-6**

Smith, J.R., Satake, K., and Suyehiro, K., 2002. Deepwater multibeam sonar surveys along the southeastern Hawaiian ridge: guide to the CD-ROM. In Takahashi, E., Lipman, P.W., Garcia, M.O, Naka, J., and Aramaki, S. (Eds.), Hawaiian Volcanoes: Deep Underwater Perspectives. Geophysical Monography, 128: 3–9. **https://doi.org/10.1029/GM128p0003**

Taylor, B., 2019. Shoreline slope breaks revise understanding of Hawaiian shield volcanoes evolution. Geochemistry, Geophysics, Geosystems, 20(8):4025–4045. **https://doi.org/10.1029/2019GC008436**

Thompson, W.G., and Goldstein, S.L., 2005. Open-system coral ages reveal persistent suborbital sea-level cycles. Science, 308(5720):401–404. **https://doi.org/10.1126/science.1104035**

Watts, A.B., 1978. An analysis of isostasy in the world's oceans, 1. Hawaiian-Emperor Seamount Chain. Journal of Geophysical Research: Solid Earth, 83(B12):5989–6004. **https://doi.org/10.1029/JB083iB12p05989**

Webster, J.M., Ravelo, A.C., and Grant, H.L.J., 2023. Expedition 389 Scientific Prospectus: Hawaiian Drowned Reefs. International Ocean Discovery Program. **https://doi.org/10.14379/iodp.sp.389.2023**

Webster, J.M., Braga, J.C., Clague, D.A., Gallup, C., Hein, J.R., Potts, D.C., Renema, W., Riding, R., Riker-Coleman, K., Silver, E., and Wallace, L.M., 2009. Coral reef evolution on rapidly subsiding margins. Global and Planetary Change, 66(1–2):129–148. **https://doi.org/10.1016/j.gloplacha.2008.07.010**

Webster, J.M., Clague, D.A., Riker-Coleman, K., Gallup, C., Braga, J.C., Potts, D., Moore, J.G., Winterer, E.L., and Paull, C.K., 2004. Drowning of the -150m reef off Hawaii: a casualty of global meltwater pulse 1A? Geology, 32(3):249–252. **https://doi.org/10.1130/G20170.1**

Webster, J.M., and Davies, P.J., 2003. Coral variation in two deep drill cores: significance for the Pleistocene development of the Great Barrier Reef. Sedimentary Geology, 159(1–2):61–80. **https://doi.org/10.1016/S0037-0738(03)00095-2**

Webster, J.M., Wallace, L., Silver, E., Applegate, B., Potts, D., Braga, J.C., Riker-Coleman, K., and Gallup, C., 2004. Drowned carbonate platforms in the Huon Gulf, Papua New Guinea. Geochemistry, Geophysics, Geosystems, 5(11). **https://doi.org/10.1029/2004GC000726**

Webster, J.M., Wallace, L., Silver, E., Potts, D., Braga, J.C., Renema, W., Riker-Coleman, K., and Gallup, C., 2004. Coral-gal composition of drowned carbonate platforms in the Huon Gulf, Papua New Guinea; implications for lowstand reef development and drowning. Marine Geology, 204(1):59–89. **https://doi.org/10.1016/S0025-3227(03)00356-6**

Webster, J.M., Wallace, L.M., Clague, D.A., and Braga, J.C., 2007. Numerical modeling of the growth and drowning of Hawaiian coral reefs during the last two glacial cycles (0–250 kyr). Geochemistry, Geophysics, Geosystems, 8(3):Q03011. **https://doi.org/10.1029/2006GC001415**

Woodroffe, C.D., and Webster, J.M., 2014. Coral reefs and sea-level change. Marine Geology, 352:248–267. **https://doi.org/10.1016/j.margeo.2013.12.006**

Yokoyama, Y., Esat, T.M., and Lambeck, K., 2001. Coupled climate and sea-level changes deduced from Huon Peninsula coral terraces of the last ice age. Earth and Planetary Science Letters, 193(3):579–587. **https://doi.org/10.1016/S0012-821X(01)00515-5**

Yokoyama, Y., Esat, T.M., Thompson, W.G., Thomas, A.L., Webster, J.M., Miyairi, Y., Sawada, C., Aze, T., Matsuzaki, H., Okuno, J., Fallon, S., Braga, J.-C., Humblet, M., Iryu, Y., Potts, D.C., Fujita, K., Suzuki, A., and Kan, H., 2018. Rapid glaciation and a two-step sea level plunge into the Last Glacial Maximum. Nature, 559(7715):603–607. **https://doi.org/10.1038/s41586-018-0335-4**

Yokoyama, Y., Lambeck, K., De Deckker, P., Esat, T.M., Webster, J.M., and Nakada, M., 2022. Towards solving the missing ice problem and the importance of rigorous model data comparisons. Nature Communications, 13(1):6261. **https://doi.org/10.1038/s41467-022-33952-z**